THE UNIVERSITY OF MANITOBA

A MASS FLOWMETER FOR PARTICULATE SOLIDS

by

MUHAMMAD SHAFI SABIR

A Thesis

Submitted To The Faculty Of Graduate Studies

In Partial Fulfillment Of The Requirements For The Degree

Of Master of Science

DEPARTMENT OF AGRICULTURAL ENGINEERING

WINNIPEG, MANITOBA

February 1976

"A MASS FLOWMETER FOR PARTICULATE SOLIDS"

by

MUHAMMAD SHAFI SABIR

A dissertation submitted to the Faculty of Graduate Studies of the University of Manitoba in partial fulfillment of the requirements of the degree of

MASTER OF SCIENCE

IN THE NAME OF ALMIGHTY GOD,

THE MAGNIFICENT, THE MERCIFUL.

ABSTRACT

This research was conducted as a second phase of investigations of capabilities and limitations of microwave Doppler radar as a flow monitor for particulate solids. Experiments were performed to extract information from the Doppler signal about the average bulk density of particulate solids, an important parameter in monitoring the mass flow rate. Different flow fields were employed including the circular and ring cross-section flow fields to study the effect of the distribution of solid material in the flow field. Monostatic free space configuration was used throughout the experiments.

Two different Doppler signal processing systems, namely, an analog (on line), and a digital (off line), were used to determine the RMS values of the Doppler signals and hence radar cross-sections of columns of wheat, moving through a plastic pipe. A commerically available tape recorder was used for recording Doppler signals from the bulk flow of granular materials and metallic calibrating spheres. The recorded data were subsequently processed by a digital computer. Radar cross-sections of various metallic calibrating spheres were determined theoretically as well as experimentally and used for calibration of the radar system. A computer program was developed for analysis of Doppler signals.

The relationship between the average bulk density of the column of wheat moving continuously through a pipe and RMS values of Doppler signals and hence their radar cross-sections was developed and verified experimentally. Experimental results of radar cross-section as a function of the average bulk density of wheat are presented.

As a result of this research it was concluded that a Doppler radar, used as a flow monitor, has an excellent capability for monitoring the flow rate of particulate solids without disturbing the monitored system. When the cross-section area of the flow field is known, this flowmeter can be used to monitor the mass flow rate of particulate solids continuously with good accuracy and without causing any obstruction in the flow field.

ACKNOWLEDGEMENTS

The author wishes to express his deepest appreciation to Dr. S. S. Stuchly for his guidance, counsel and patience as a major professor during the course of this project. Thanks are due to Dr. M.A. Rzepecka for many valuable suggestions and help in every way possible.

Appreciation is extended to Professors J.S. Townsend and R.S. Azad for reviewing the manuscript as the examination committee members.

Analysing data for this study was an enormous job. I sincerely appreciate the valuable suggestions and sincere help extended by Mr. Neil-Jon Morphy for analysis of data on a digital computer.

I am especially grateful to the Manitoba Department of Agriculture and the Faculty of Graduate Studies for their financial support of this project.

I am indebted to my parents for their encouragement and humble prayers to God from thousands of miles across the sea.

Special thanks are due to Mrs. Darlene Lowry for her tireless efforts in typing this manuscript.

TABLE OF CONTENTS

LIST OF FIGURES

LIST OF TABLES

LIST OF SYMBOLS

A_{av}	Average cross-sectional area of the flow field
A_e	Equivalent antenna aperture
A_{RMS}	RMS value of the Doppler signal scattered by a target
$A_{o_{RMS}}$	RMS value of the Doppler signal scattered by a calibrating sphere
D	Kernel density of a single particle
D_{av}	Average bulk density
E_i	Magnitude of the incident electric field
E_r	Magnitude of the reflected electric field
F	Shape factor
$\|K\|^2$	A factor which depends upon the electromagnetic properties of the flow field
L	Elongation factor
L_a	Length of the flow field in the direction of antenna beam
M	Moisture content
M_{av}	Average mass flow rate
N	Number of particles
N_s	Number of samples
P_r	Power received
P_t	Power transmitted
P_{ro}	Power scattered by a calibrating sphere
R	Radar range
$S_x(f)$	Frequency content of a time varying signal
T	Time period of flow
T_1	Temperature
T_w	Time window
U	Velocity component

V	Volume of the target
V_{av}	Average velocity of the flow field
W_R	Uncertainty in the result
W	Weight of the material
$W_{D_{av}}$	Uncertainty in the average bulk density
$X(t)$	Time dependent signal
a	Correction factor
a_o	Radius of the sphere
c	Velocity of propagation of electromagnetic waves
c_o	Velocity of sound waves in the fluid
d	Diameter of a single particle
e	A factor defining the third axis of a spheroid
f	Value of data points
f_o	Frequency of transmission
f_d	Doppler frequency
f_{di}	Instantaneous Doppler frequency
h	Altitude of right circular cone
n	Constant time interval between consecutive data points
v	Velocity of the target
w_1	Uncertainty in the weight of material
w_2	Uncertainty in the time period of flow
w_3	Uncertainty in measurement of velocity
w_4	Uncertainty in measurement of cross-sectional area of the flow field
x_1, x_{n-1}, x_n	Independent variables

Δf_d	Bandwidth of the Doppler frequency spectrum
$\Delta\theta_2$	Two way 3dB antenna beamwidth
Δt	Time interval between samples
$\Delta\omega$	Difference between the transmitted and the received angular frequencies
Δd	Error in measurement of the diameter of sphere
α	Angle between the transmitting beam and the direction of the velocity vector
β	Angle between the receiving beam and the direction of the velocity vector
ε'	Dielectric constant
ε''	Loss factor
θ	Viewing angle
λ	Free space wavelength
σ	Backscattering radar cross-section of the target
σ_{av}	Average radar cross-section of the target
σ_o	Radar cross-section of the calibrating sphere
δ_{f_d}	Standard deviation of the instantaneous Doppler frequency
ω	Angular frequency of the scattered sound wave
ω_o	Angular frequency of the incident sound wave
RCS	Radar cross-section
RMS	Root mean square value

CHAPTER I

INTRODUCTION

The subject of flow metering of particulate solids dates back a few decades. Several efforts have been made in the past to design and develop practical flowmeters for monitoring the mass flow rate of granular materials. However, none of the flowmeters developed so far, proved to be suitable for applications, which require an inexpensive and accurate flowmeter for measuring the mass flow rate of particulate solids. With the advancement in agricultural technology, and other areas of engineering, there has been an increasing need for some means of measuring flow rates of particulate solids. From harvesting of grain to the point of consumption, a flowmeter may potentially play an important role in enabling the Government authorities to obtain more accurate and earlier estimates of national yield, which would be helpful in planning and have a settling effect on the new cereal market. The information obtained would also be helpful to individual farmers who could compare their yields arising from different grain varieties, fertilizer applications, cultivations techniques etc., and could plan their future contracts more accurately. Flowmeters are also needed to weigh grain as it is loaded onto trucks or ships or delivered into grain driers. In sugar, fertilizer, cement, paper and other chemical industries there has been a growing need for a measuring device for solid materials, because of the fact that the quality of the final product and the performance of the plant depend to a large extent upon precise measurements.

Several flowmeters, based on various principles of operation, have been developed in the past. By far, continuous weighing is one of the most commonly utilized methods of measuring the flow rates of particulate

solids. The principle of change of angular momentum of the measured material has also been utilized by different authors to monitor the mass flow rate of granular materials. A spiral vane flowmeter, for measuring the volumetric flow rate of particulate solids moving through vertical ducts, is another reported device. Optical methods for detecting and measuring the volumetric flow rates of powders have been practised in the past. Nucleonic methods for monitoring the mass flow rate of granular solids, is another contribution towards the solution of this problem. Recently, laser anemometers and ultrasonic flowmeters have been introduced for measuring the velocity of flow fields, without introducing any mechanical probe into the flow field. The microwave Doppler flowmeter technique for particulate solids was first suggested by Ellerbruch and Parker. Harris made some qualitative studies on applications of this technique to the flow metering of particulate solids. The first quantitative studies of this technique were made by Hamid to monitor velocity of granular materials falling freely under gravity. The detailed review of the subject is presented in Chapter II.

During the last few years, the increasing demand for more accurate solid flow measurements has exceeded the capability of the existing flowmeters for particulate solids. None of the existing flowmeters, however, is suitable for the applications, which require a compact, inexpensive device to measure a high flow rate continuously, and without causing any obstruction in the conveying system.

The aim of this work was to investigate further capabilities and limitations of the Doppler radar flowmeter for continuous and contactless measurements of particulate solids. The particular objective of this work was to analyse the Doppler signal and to retrieve useful information

about the average bulk density of the granular materials moving through a pipe. When the cross-sectional area of flow is known, the average mass flow rate can be determined easily by multiplying the average bulk density by the average bulk velocity and by the cross-section area of the flow field.

CHAPTER II

REVIEW OF LITERATURE

Monitoring mass flow rate of particulate solids with high accuracy has been a major problem in many areas of engineering. The complete solution awaits mainly the development of an accurate mass flowmeter, which is by no means a trivial task. A brief review is given here indicating the basic problems in monitoring the mass flow rate of granular materials and some of the contributions made in its solution. The capabilities and limitations of microwave Doppler flow monitor and other noncontact flow measuring systems, for example, ultrasonic flowmeters and laser anemometers are discussed in some detail.

Although the basic principles used for monitoring the mass flow rate of fluids apply equally well to granular materials, typical sensors usually obstruct the flow of the material, change the flow pattern, assist the formation of blockages and therefore limit practical use of the modified forms of fluid flowmeters for granular materials. The relatively high resistance to shear forces of granular material compared to that of fluids further explains the lag of flow measurement techniques for granular materials. However, a few devices and techniques exist to measure the flow rate of particulate solids. None of the existing flowmeters is suitable for applications which require a compact, inexpensive and noncontact device for measurements at high flow rates in difficult, hostile environments and inaccessible situations.

Flowmeters based on the principle of weighing the material continuously are the most common devices for monitoring the mass flow rate of granular and powdered materials. The material passing a fixed point on a conveyor belt or through a hopper can be weighed. (Beck et al., 1969).

Early methods of weighing on a conveyor belt contained a pivoted arm restored to the equilibrium position by weights. The restoring force was thus proportional to the weight of material on the belt. (Kirwan and Demler, 1955). Modern instruments employ load cells to measure the weight of the material on the belt, and a tachometer generator to measure the speed of the belt. (Valenti, 1961 and Craven, 1964). Continuous weighing is an accurate method of measuring solid flow rates on a belt conveyor. As these flowmeters contain moving parts, a fair amount of care is required to maintain the required accuracy. These methods are not in general suitable for pneumatic conveyors.

The principle of momentum change of the measured material has also been used in the past to measure the mass flow rate of particulate solids. A flowmeter working on this principle has been developed and reported. (Dean, 1955). The meter incorporates an inclined plate attached to a rigid beam, pivoted about a point near its centre. The material falls onto the inclined plate and the moment is measured by a force balance unit. If the velocity of the material is constant, the force on the plate is proportional to the mass flow rate. This device, however, can only be used for dense materials, falling freely under gravity. Moreover, it can cause obstruction in the conveying system. Recently, a combine harvester discharge meter employing the same principle has been developed in NIAE, Silsoe. (Hooper et al., 1973). The meter incorporates an impact plate in the form of a funnel through which the grain falls, and the force exerted on the funnel is a measure of the flow rate of grain. The meter gave good results for wheat and rather poor results for barley. The poor results for barley may be due to formation of blockages in the conveying system because freshly harvested barley is usually not clean and may contain roughages. This

device can only be used for materials of large density and is not suitable for materials of small density due to the buoyancy forces effect. Furthermore, the impact plate can cause blockages in the conveying system.

Rotating impeller flowmeters working on the principle of the change of angular momentum of the measured material have also been developed and reported. The torque produced in the supporting shaft due to the change in the angular momentum is a measure of the mass flow rate. A mass flowmeter based on this principle has been developed and reported. (Henderson, 1966). This device consists of an impeller with eight vertical vanes rotating at a constant speed, which is driven by a synchronous motor clamped to the impeller shaft. The reaction torque on the motor produced by solids flowing through the impeller is transmitted to the shaft by a clamp. This causes the shaft to twist, and the torque is measured by a system with four strain gages. A flowmeter working on the same principle was also reported earlier. (Kirwan and Demler, 1955). Rotating impeller flowmeters can only be used in ducts where the solid material is falling freely under gravity. Moving parts of the system require considerable maintenance, particularly when abrassive powders are being conveyed. Furthermore, the flowmeter is a potential source of obstruction in the conveying system.

Optical methods can be used to measure volumetric flow rates of powders (Beck and Wainwright, 1969). These methods of flow measurement are volumetric and make no allowance for variations in the packing density of the material. They can be used only with materials having high reflection coefficients and their accuracy can be seriously affected by dust settling on optical windows.

A spiral vane flowmeter measures directly the volume of granular solids moving through a spiral vane (Brown et al., 1962). The spiral vane is connected to a revolution counter, and the number of revolutions due to moving granular solids through the duct, is a direct measure of the volumetric flow rate. This device can only be used in ducts greater than 25 cm (10 in) in diameter, which should not be tilted more than 20° from the vertical plane.

Nucleonic methods for monitoring the mass flow rate of granular solids utilize the fact that the radiation absorbed by the material depends on the mass of the material in the path of the radiation. A flowmeter employing this principle was reported. (Perkovski, 1963). In this meter the grain is flowing through a specially Z-shaped bend and the radiation absorption of the material in the bend is measured. This flowmeter can be used successfully with belt conveyors if belt velocities can be measured readily. It can also be used in pneumatic conveyors if the velocity of the flow is measureed independently.

The electromagnetic flowmeters are based on Faraday's law of electromagnetic induction. When a conductive liquid flows, the voltage induced is proportional to the average velocity of the liquid, the strength of the magnetic field, and the distance between the electrodes. In a given meter, the magnetic field and the distance between the electrodes are usually designed to remain constant; therefore, the induced voltage is directly proportional to the flow velocity. The flowmeters working on this principle have been reported and marketed by a number of companies (Webb, Stone and Webster, 1974). These flowmeters can measure the flow of blood, slurries, corrosive liquids, viscous materials, milk and pharmaceuticals. Electromagnetic flowmeters are obstructionless and

contain no moving parts, but work satisfactorily only for conductive materials.

Recently, laser anemometry have been introduced for measuring the flow velocity of fluids without introducing any mechanical probe into the flow field. Several anemometer systems have been used, the differences being basically in the optical configuration and the signal processing schemes used. (DISA, 1973). The fluid velocity is measured by measuring the Doppler shift of laser radiation scattered by small particles moving in the fluid flow. A flowmeter based on this technique was first developed and reported by Yeh and Cummins (1964). This laser Doppler anemometer focuses two light beams in such a manner that they intersect in the flow field at their focal points. The frequency of the light wave from the illuminating beam scattered by the moving particles towards the photo-multiplier is shifted by (Goldstein and Kried, 1967)

$$f_d = 2U \sin \theta/\lambda$$

where λ is the wave length and θ is the viewing angle, both measured in the fluid. The U component of velocity is determined either from direct measurement of the photocurrent frequency, or from the spectrum of the photocurrent. Although laser anemometers have excellent capabilities for measuring supersonic flows, local velocities without disturbing the flow, and are characterized by high spacial resolution and low uncertainity in measurement, they cannot be used to monitor the flow rate of particulate solids.

Flowmeters based on the Doppler effect of ultrasound have also been developed and reported by different authors. Here the Doppler priniciple is used for measuring the velocity of fluids. The Doppler

effect appears when the ultrasound wave strikes a moving particle. The particle scatters the sound wave in all directions. The frequency of the scattered sound wave differs from the frequency of the incident sound wave by $\Delta\omega$.

$$\Delta\omega = \omega - \omega_o = \frac{\omega_o}{c_o} v \, (\cos \alpha + \cos \beta)$$

where ω is the angular frequency of the received signal, ω_o is the angular frequency of the transmitted signal, c_o is the velocity of sound in the medium, v is the velocity of the particle, α is the angle between the transmitting beam and the direction of the velocity vector of the particle and β is the angle between the receiving beam and the direction of the velocity vector of the particle. A flowmeter working on this principle has been reported (Arts and Roevros, 1971) for measuring blood flow rates. It has been found that the received signal contained a spectrum of frequencies and not a single discrete frequency, because of the various velocities of the scattering particles, depending on their relative positions in the blood vessel. The authors concluded that the instantaneous Doppler frequency does not give meaningful information about the blood flow. The Doppler frequencies have to be averaged over a certain period of time in order to obtain quantitative information about the blood flow rate. Another flowmeter working on the same principle and used for the diagnosis of urethral parameters has been developed recently (Albright and Harris, 1975). Despite the fact that ultrasonic flowmeters are contactless and can measure the parameters of fluid flow without distrubing the monitored system, they cannot be easily employed for monitoring the velocity of the flow of particulate solids.

The microwave Doppler flowmeter technique for particulate solids

was first suggested and reported by Ellerbruch (1970) and Parker (1970). Harris (1970), made some *qualitative* studies of this technique when applied to the flow metering of particulate solids. A Doppler radar as a flow monitor for detection of flow failures in granular or powder flow was suggested by Hannir (1970). The *quantitative* studies of this technique for measuring the mass flow rate of particulate solids were first made and reported by Hamid (1975). He found that the frequency of the Doppler signal from single scattering particles was spread over a finite bandwidth and that the mean frequency of the Doppler spectrum was proportional to the mean velocity of the flow field. Further investigations showed that due to the semi-random movements of particles in the flow field and due to multiple scattering from particles in the flow field the resulting Doppler signal had a complex wave form. The signal had to be averaged in order to extract the desired information about the average bulk velocity of the granular material. If the cross-section area of the flow field and material density are known, the average bulk velocity is proportional to the average mass flow rate.

The review of the technical literature on the subject clearly shows that none of the existing flowmeters is suitable for applications which require an inexpensive and noncontact and nonobstructing flowmeter for monitoring the mass flow rate of particulate solids. The microwave Doppler flowmeter seems to have all the capabilities required for monitoring the parameters of the flow field and shows considerable potential for the solution of this important measurement problem.

CHAPTER III

THEORETICAL CONSIDERATIONS

3.1 Introduction

Knowledge of the fundamental equation for mass flow rate is essential in designing and developing of a flowmeter for particulate solids. For example, in monitoring mass flow rate of granular materials, the average bulk velocity, the average bulk density and the average cross-section area of the flow field should be known to determine the mass flow rate.

In this chapter the basic equation for the mass flow rate of particulate solids, will be given and the radar cross-section (RCS) of a single scattering particle and multiple scattering particles will be discussed. The relationship between the RMS value of the Doppler signal and the average bulk density of particulate solids as well as the relationship between the RCS and the average bulk density will be described. The principle of measurement of the average Doppler frequency, the Fast Fourier Transform (FFT) and the power spectrum of the Doppler signal waveform will also be presented. Diagrams of the Doppler waveform and power spectrum are given and discussed to develop better understanding of the experimental results discussed in Chapter V.

3.2 Mass Flow Rate

The fundamental equation for the average mass flow rate of particulate solids can be formulated as follows:

$$M_{av} = A_{av} \times D_{av} \times V_{av} \qquad (3.1)$$

where M_{av} is the average mass flow rate in kg/sec, D_{av} is the average bulk density of the flowing material in kg/m^3, V_{av} is the average bulk

velocity of the material in m/sec, A_{av} is the average cross-section area (m^2) of the moving column of grain determined by the interaction between the flow field and the beam of the electromagnetic waves.

3.3 Doppler Radar as a Mass Flow Monitor

The microwave Doppler flowmeter technique was first introduced by Ellerburch (1970) and Parker (1970). Harris (1970) made some qualitative studies on applications of this technique to the flow metering of particulate solids. Hannir (1970) suggested the use of the Doppler radar principle for detection of the flow failures in the flow of granular or powdered materials.

The average RMS value of the Doppler response carries information about the average bulk density of the moving material. The relationship between the average RMS value of the Doppler signal and the average bulk density of particulate solids will be discussed in section 3.4. The average Doppler frequency bears information about the average bulk velocity of the flowing particulate solids (Hamid, 1975). The antenna beam is usually divergent and has a finite beamwidth $\Delta\theta_2$ as shown in Fig. 3.1, therefore, a spectrum of frequencies results as shown in Fig. 3.3(b) and the Doppler spread is given by (Hyltin et al., 1973)

$$\Delta f_d = \frac{2v}{\lambda} \left[\cos\left(\theta - \frac{\Delta\theta_2}{2}\right) - \cos\left(\theta + \frac{\Delta\theta_2}{2}\right)\right] \qquad (3.2)$$

where Δf_d is the Doppler spread in Hz, v is the velocity of the target in m/sec, λ is the free space wavelength in m, θ is the viewing angle and $\Delta\theta_2$ is the two way 3dB beamwidth.

Although the frequency of the Doppler signal from a single scattering particle is spread over a finite bandwidth, it was found that the mean frequency of the Doppler spectrum gives an accurate value of

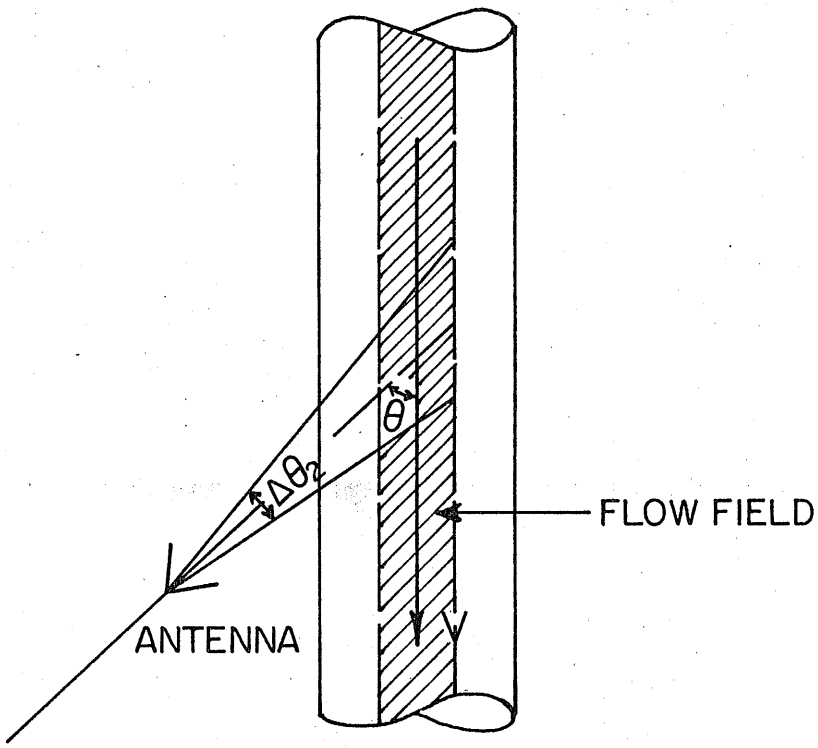

Figure 3.1 Flow Field and Antenna Beam Geometries

the average velocity for a given viewing angle (Hamid, 1975).

The average cross-section area of the flow field is determined by interaction between the electromagnetic waves and the flow field and is a constant factor which depends upon the calibration of the flowmeter. The microwave Doppler flowmeter monitors the parameters of the flow field without causing any obstruction in the flow path of the material.

3.4 Relationship Between the RMS Value of the Doppler Signal and the Bulk Density

Plane electromagnetic waves travelling through the space containing particles of solid materials are scattered and absorbed by these particles. The scattered (radar) signal from the particles of a granular material is not steady like that from a point scatterer or target. The received (back-scattered) signal at any instant is composed of signals from a very large number of particles, and depends on their exact arrangement in space, which is continuously changing. Studies of scattering and attenuation by meteorogical particles (Marshall and Hitschfeld, 1953), have shown that instantaneous observations of the received power give very little information about the scattering medium, and the signal has to be averaged until a large number of independent returns have been received. The average power scattered by the flow field is

$$P_r = \frac{P_t \cdot A_e \cdot L_a}{8\pi R^2} \Sigma\sigma \qquad (3.3)$$

where P_t is the transmitted power, A_e is the equivalent antenna aperture, L_a is the length of the flow field in the direction of the antenna beam, R is the distance from the point of observation to the flow field and $\Sigma\sigma$ is the equivalent radar cross-section of the flow field.

The equivalent aperture A_e is less than the actual area of the antenna for two reasons. Firstly, not all the power coming from the primary feed falls inside the antenna aperture, neither is the distribution of power uniform across the aperture because the amplitude of the signal varies due to the variations in the distance to the target and intensity of radiation which depends upon the antenna pattern. The amplitude of the signal increases as the target approaches the antenna axis. The peak of the signal occurs in the region where the ratio of the radiation intensity to the fourth power of range is maximum. It decreases again as the target recedes, because of decreasing radiation intensity off the antenna axis. The second reason, which applies only to distributed targets, affects radar systems. Some of the radiated power goes into side lobes and the edges of the main beam, and some of the returned power comes from directions to which the antenna is less sensitive for reception. An exact value for A_e is difficult to determine but a conservative estimate is probably 0.5 x actual area.

The equivalent radar cross-section depends upon the geometrical and electromagnetic properties of the flow field. For wavelengths large compared with the diameter, d , of the particles, the RCS of a single particle can be expressed as follows (Skolnik, 1962)

$$\sigma = \frac{\pi^5 d^6}{\lambda^4} |K|^2 \qquad (3.4)$$

where λ is the free space wavelength, d is the diameter of the scattering particles and $K = \frac{m^2-1}{m^2+2}$, while $m = \sqrt{\varepsilon' - J\varepsilon''}$ where ε' is the dielectric constant and ε'' is the loss factor of the scattering particles.

The relationship between the dielectric constant and the density

of wheat and the loss factor and density of wheat can be expressed as follows (Nelson, 1972)

$$\varepsilon' = 1.2283 + 0.8480\,D + 1.2180\,D^2 \tag{3.5}$$

$$\varepsilon'' = .8508 - 1.9150\,D + 1.4373\,D^2 \tag{3.6}$$

where D is the kernel density of a single particle in g/cm^3. Combining eqs. 3.3 and 3.4

$$P_r = \frac{\pi^4 \cdot P_t \cdot A_e \cdot L_a}{8R^2 \cdot \lambda^4} \Sigma\, d^6\, |K|^2 \tag{3.7}$$

where symbols are the same as in eqs. 3.3 and 3.4.

From eq. 3.7 it can be concluded that since all the parameters are constant for a particular Doppler module except the dielectric properties of the flow field, therefore, the received power is a function of the dielectric properties of the flow field. Further the dielectric properties of the flow field depend on the density, moisture content, and temperature of the flowing material. Although both the moisture content and temperature of the granular material affect its dielectric properties and, therefore, the received power, this is believed to be much weaker than the effect of density. This will be discussed in detail in section 3.6.

3.5 Radar Cross-section

3.5.1 Single Scattering Particle

The radar cross-section of a target may be defined as the area intercepting that amount of power which, when scattered equally in all directions, produces an echo at the radar equal to that from the target (Skolnik, 1962), or in mathematical terms

$$\sigma \underset{R \to \infty}{=} 4 \pi R^2 \left| \frac{E_r}{E_i} \right|^2 \qquad (3.8)$$

where R is the distance between the radar and the target, E_r is the reflected field strength, E_i is the strength of the incident field.

Theoretically, the scattered field, and hence the radar cross-section, can be determined by solving Maxwell's equations with the proper boundary conditions applied, but this method is applicable only for the simplest shapes. The radar cross-section is frequency dependent. The region where the size of the sphere is small compared with the wavelength, ($2\pi a_o/\lambda << 1$), where a_o is the radius of the sphere in m and λ is the wavelength in m) is called the Rayleigh region. At the other extreme from the Rayleigh region is the optical region, where the dimensions of the sphere are large compared with the wavelength that is $2\pi a_o/\lambda >> 1$. Between the optical and the Rayleigh region is the Mie, or resonance region. The RCS is oscillatory with frequency within this region. The radar cross-section for most of the particulate solids of interest falls in the Rayleigh region and, therefore, the discussion that follows, is limited to this region.

The RCS of an object depends upon

1. the size of the object
2. the frequency of the incident radiation
3. the polarization of the transmitting antenna
4. the orientation of the object relative to the plane of polarization
5. the material of which the object is made, and
6. the shape of the object.

The critical parameter in the Rayleigh region is the volume of the scattering object. RCS for all spheroids with semi-axes a, a, and b,

the Rayleigh RCS for backscattering along the axis of symmetry ($\theta=0$) is given by (Crispin and Maffet, 1965)

$$\sigma = \frac{4}{\pi} K^4 V^2 F^2 \left[1 + \frac{1}{\pi y} e^{-y}\right]^2 \tag{3.9}$$

where σ is the radar cross-section in m^2, $K = 2\pi/\lambda$, λ is the free space wavelength in m, V is the volume of the object in m^3, F is the shape factor, and $y = b/a$.

Except for very flat oblate spheriods the quantity in the brackets can be neglected.

The shape factor F is equal to

$$F_{\text{horz. pol.}} = \frac{1}{2}\left[\frac{1}{2 - L} + \frac{\cos^2\theta}{L} + \frac{\sin^2\theta}{2 - 2L}\right] \tag{3.10}$$

$$F_{\text{ver. pol.}} = \frac{1}{2}\left[\frac{1}{L} + \frac{\cos^2\theta}{2 - L} + \frac{\sin^2\theta}{2L}\right] \tag{3.11}$$

and

$$L_{\text{(prolate spheriod)}} = \frac{1}{e^2} - \frac{1 - e^2}{2e^3} \ln\frac{1 + e}{1 - e} \tag{3.12}$$

where, the semi-axis are a, a, $\frac{a}{\sqrt{1 - e^2}}$

$$L_{\text{sphere}} = \frac{2}{3}$$

$$L_{\text{oblate spheroid}} = \frac{\sqrt{1 - e^2}}{e^3} \sin^{-1} e - \frac{1 - e^2}{e^2} \tag{3.13}$$

where the semi-axis are a, a, $a\sqrt{1 - e^2}$. For a sphere the shape factor F, at all polarizations and viewing angles is constant and is equal to 1.125.

Since the critical parameter of the scatterer in the Rayleigh region is its volume, it is natural to consider the application of the expressions just mentioned for spheroids to all bodies of revolution. Of course, this extension requires careful consideration of the parameter y. To illustrate this, let us consider a right circular cone of altitude h and base radius a. For the limiting case in which the right circular cone collapses into a disk of radius a i.e., the limit as $h \to 0$, we find that the appropriate ratio is given by $y = h/4a$. Hence, the cone has the same RCS as a spheroid of equal volume whose semi-axes are a, a and $h/4$.

3.5.2 Multiple Scattering Particles

As discussed in 3.5.1 eq. 3.9 applied to calculate the radar cross-section of spheroids can be extended equally well to determine the RCS of all bodies of revolution. But the most common method of determining the RCS of an object is the comparison method in which the power scattered from the object is compared with the power scattered from a standard located in the same position as the actual object. This method eliminates the problem of the sensitivity of the radar since the RCS of the standard (metallic sphere) can be easily calculated analytically. Therefore, it is only necessary to measure the ratio of the power scattered from the two targets. The RCS of a given object can then be calculated easily. Under similar conditions, the ratio of power received is

$$\frac{P_r}{P_{ro}} = \frac{\sigma}{\sigma_o}$$

but

$$\frac{P_r}{P_{ro}} = \frac{(A_{RMS})^2}{(Ao_{RMS})^2}$$

therefore,

$$\frac{\sigma}{\sigma_o} = \frac{(A_{RMS})^2}{(Ao_{RMS})^2} \tag{3.14}$$

where σ is the radar cross-section of the target in m^2, σ_o is the RCS of the calibrating sphere in m^2, A_{RMS} is the RMS value of the signal scattered by a given target in V and Ao_{RMS} is the RMS value of the signal scattered by the calibrating sphere in V.

3.6 Relationship Between RCS and Density

The scattering by multiple particles (bulk flow of particulate solids) represents a much more complicated case as compared to a single scattering particle. The number of particles illuminated and their orientation with respect to the antenna beam both affect the equivalent RCS. For simplicity of calculations, it is assumed that the scattering medium (grains) consists of a collection of identical independent scatterers that scatter isotropically. The number of scattering particles at any time is changing very slightly.

The RCS of a single scattering dielectric particle can be expressed by eq. 3.4

$$\sigma = \frac{\pi^5 d^6}{\lambda^4} |K|^2 \tag{3.15}$$

where symbols carry the same meaning as in eq. 3.4.

If the volume under consideration contains N particles, the average RCS is formulated as follows (Skolnik, 1962)

$$\sigma_{av} = \frac{\pi^5}{\lambda^4} \sum_{i=1}^{N} d^6 |K|^2 \tag{3.16}$$

Using eqs. 3.5 and 3.6, $|K|^2$ can be written as

$$|K|^2 = \frac{.775 - 2.871\,D + 7.387\,D^2 - 3.438\,D^3 + 2.065\,D^4}{11.145 + 2.217\,D + 14.695\,D^2 - 3.438\,D^3 + 3.549\,D^4} \qquad (3.17)$$

Substituting value of $|K|^2$ in eq. 3.16

$$\sigma_{av} = \frac{\pi^5}{\lambda^4} \sum_{i=1}^{N} d^6 \left[\frac{.775 - 2.871\,D + 7.387\,D^2 - 3.438\,D^3 + 2.065\,D^4}{11.145 + 2.217\,D + 14.695\,D^2 - 3.438\,D^3 + 3.549\,D^4}\right] \qquad (3.18)$$

where σ_{av} is the average RCS of N particles in cm^2, D is the kernel density for a single wheat grain in g/cm^3, λ is the free space wavelength in cm.

As discussed in section 3.4 the average power scattered back and hence the RCS depend on the dielectric properties of the flow field, and, therefore, density, moisture content, and temperature. The effect of the moisture content and temperature is, however, much weaker than the effect of the density. For illustration the following example is considered.

The values of the RCS for wheat as a function of its density calculated from eq. 3.18, are plotted in Fig. 3.2 taking the equivalent diameters of wheat seed and wavelength .3328 cm and 2.85 cm respectively. The effect of moisture content of wheat on its equivalent RCS can be determined using the regression equations describing the relationship of the dielectric constant, ε' and the loss factor, ε'' with moisture content developed by (Chugh, 1973)

$$\varepsilon' = 1.953 + 0.039M \qquad (3.19)$$

$$\varepsilon'' = .249 + 0.041M \qquad (3.20)$$

where M is the moisture content in percent on wet basis.

Combining eqs. 3.5 and 3.6,

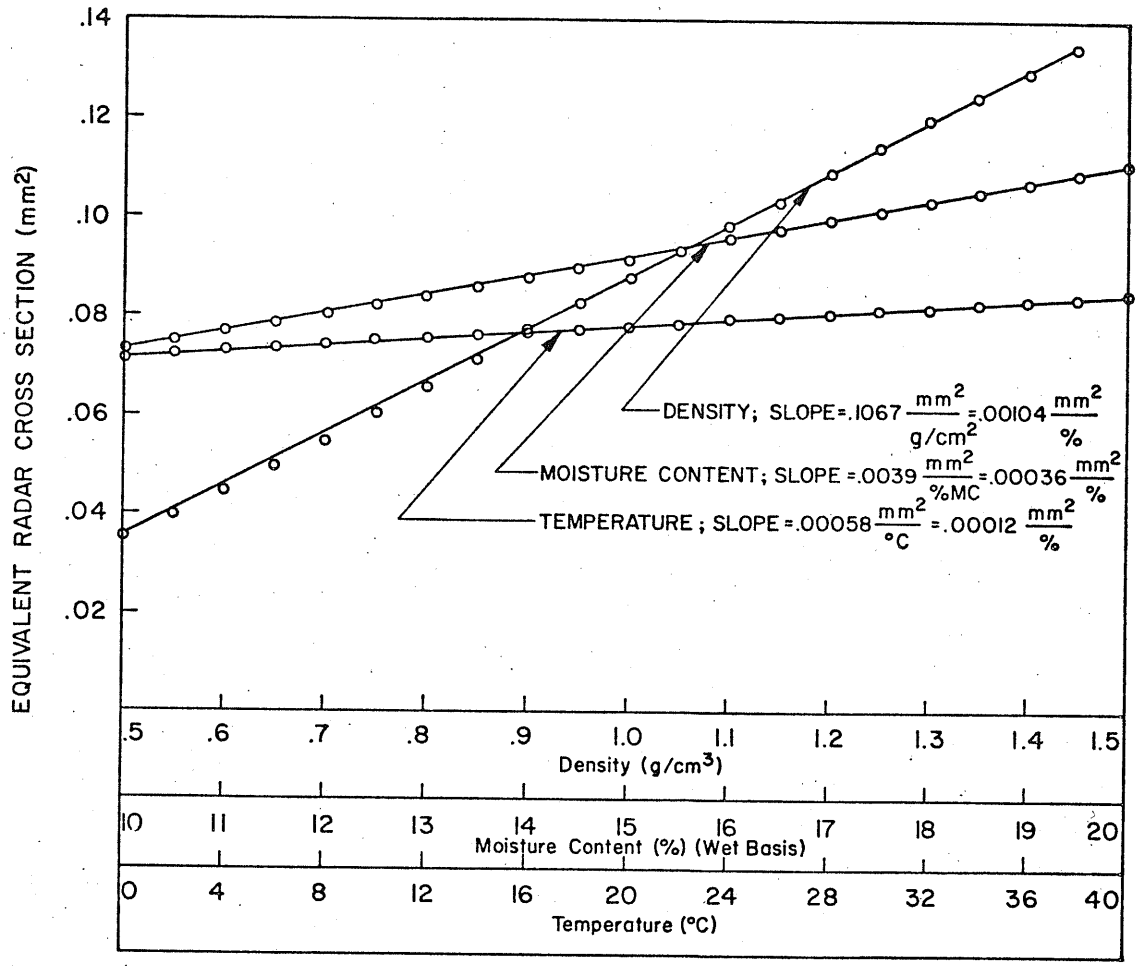

Figure 3.2 RCS for Wheat as a Function of its Density Moisture Content and Temperature. Points shown represent calculated values based on the experimental results. (Nelson, 1972 and Chugh, 1972). Straight lines represent the least squares approximations.

$$|K|^2 = \frac{.970 + 0.94M + .003M^2}{15.688 + .328M + .003M^2} \tag{3.21}$$

and substituting in eq. 3.16

$$\sigma = \frac{\pi^5}{\lambda^4} \sum_{i=1}^{N} d^6 \left[\frac{.970 + .094M + .003M^2}{15.688 + .328M + .003M^2}\right] \tag{3.22}$$

the symbols bear the same meaning as in eq. 3.16. The RCS as a function of moisture content of wheat is plotted in Fig. 3.2.

The effect of temperature of wheat on its equivalent RCS can be found by considering the following regression equations (Chugh, 1973)

$$\varepsilon' = 2.36 + .005T_1 \tag{3.23}$$

$$\varepsilon'' = .637 + .001T_1 \tag{3.24}$$

where ε' and ε'' are the dielectric constant and the loss factor of the material respectively, and T_1 is the temperature.

Using eqs. 3.5, 3.6 and 3.16

$$\sigma = \frac{\pi^5}{\lambda^4} \sum_{i=1}^{N} d^6 \left[\frac{2.190 + .014T_1 + .002T_1^2}{19.206 + .004T_1 + .0002T_1^2}\right] \tag{3.25}$$

Fig. 3.2 shows the values of RCS of wheat plotted as a function of its temperature.

Fig. 3.2 shows that the effect of density of wheat on its equivalent RCS is much larger than the effect of moisture content and temperature. Furthermore, the RCS of wheat is almost a linear function of its density.

3.7 Principle of Measurement of the Mean Frequency in the Distributed Spectrum

The determination of the mean frequency of the power spectrum of a stationary random process is a problem often encountered in a variety of

engineering applications. For example, in velocity measurement in Doppler navigation (Pawula, 1968), or in frequency measurement of a received carrier which had been transmitted through a fading medium, the mean frequency of the spectrum must be measured, since the received signal is noise-like and has some appreciable bandwidth. Various techniques such as short-time autocorrelation (Schultheiss et al., 1954), frequency discrimination or zero-crossing counting (Ehrman, 1955), correlation detection (Kobayashi, et al., 1974), frequency to voltage converter (Brody et al., 1974), are employed for the mean frequency measurement of a random signal, and the methods based on these techniques have been studied.

During the course of this research two methods were employed in order to measure the mean Doppler frequency, f_d in a distributed spectrum. In the first method the signal was passed through a frequency-to-voltage converter (analog frequency meter) producing an output voltage proportional to the Doppler frequency, which was used to measure the velocity of the flow. In the second method, which can be considered as the most accurate for measuring the average Doppler frequency, the power spectrum of the Doppler signal is computed. The power spectrum of the received signal, shows the distribution of frequencies in the backscattered signal, and contains all the information concerning the flow field. The average frequency derived from the power spectrum is proportional to the average velocity of particulate solids. The frequency at which the peak of the spectrum appears may not necessarily be the same as the average frequency, but is equal to some suitable characteristics of the power spectrum. Studies reported by Edwards et al. (1970) for signals from a laser Doppler flowmeter showed the existence of a shift of the mean Doppler frequency on the power spectrum curve.

3.8 Principle of Measurement of the RMS Value of Doppler Signal

Two basic systems can be applied to measure the RMS value of the received Doppler signal: an analog system and a digital system.

In the analog system, the Doppler signal is passed through a pass-band amplifier to boost the signal to a level convenient for processing. A true RMS voltmeter is incorporated in order to measure the RMS value of the received Doppler signal. A recorder is also used to record the RMS value of the Doppler signal for further utilization.

In the digital system, the signal is fed to a digital computer and the power spectrum of the Doppler signal is calculated. The area under the power spectrum curve gives the square of the RMS value of the Doppler signal.

3.9 The Fast Fourier Transform

The Fourier Series is a useful tool for determining the frequency content of a time-varying signal. The Fourier Transform Pair is defined as:

$$S_X(f) = \int_{-\infty}^{\infty} X(t)\, e^{-i2\pi ft}\, dt \qquad \text{(Forward Transform)} \qquad (3.26)$$

$$X(t) = \int_{-\infty}^{\infty} S_X(f)\, e^{i2\pi ft}\, df \qquad \text{(Inverse Transform)} \qquad (3.27)$$

where $e^{\pm 2\pi ft} = \cos(2\pi ft) \pm i \sin(2\pi ft)$, is known as the kernel of the Fourier Transform. $S_X(f)$ contains the amplitude and phase information at every frequency present in $X(t)$ without demanding that $X(t)$ be periodic.

An algorithm for the computation of the Fourier coefficients which requires much less computational effort was reported by Cooley and Tuckey (1965). This method is now widely known as the Fast Fourier Transform.

In digital analysis techniques for analysing a continuous waveform, the data is sampled, usually at equally spaced intervals of time, in order to produce a time series of discrete samples which can be fed into a digital computer. When these samples are equally spaced they are known as Nyquist samples. The Discrete Fourier Transform (DFT) of such a time series is closely related to the Fourier transform of the continuous waveform from which samples have been taken to form the time series. This makes the DFT particularly useful for power spectrum analysis and filter simulation on digital computers.

In order to calculate $S_X(f)$ it is necessary to take an infinite number of samples of the input waveform. As each sample must be separated by a finite amount of time, one would have to wait forever for the calculation of $S_X(f)$ to be completed. Clearly then, the observation time has to be limited in order to calculate a useful Fourier transform. It is assumed that the input signal is observed (sampled) from some zero time reference to time T_W seconds.

Then

$$\frac{T_W}{\Delta t} = N_S \tag{3.28}$$

where Δt is the time interval between samples, N_S is the number of samples, and T_W is the time window. As there are no longer an infinite number of time points, calculation of magnitude and phase values at an infinite number of frequencies cannot be expected. Equivalently, the truncated version of eq. 3.26 produces a discrete spectrum. This discrete

finite transform (DFT) is given by

$$S_X(f) = \sum_{i=o}^{N-1} X(t)\, e^{-i2\pi ft}\, dt \qquad (3.29)$$

The FFT of the Doppler signal was performed by a digital computer (PDP-11) using the software package of the computer (SPARTA).

3.10 Power Spectrum

The power spectrum of the received signal, showing the distribution of the Doppler frequencies in the backscattered Doppler signal, contains all the information about the flow field. Important information which can be obtained from the power spectrum is the mean Doppler frequency and the RMS value of the Doppler signal.

The mean Doppler frequency which is directly proportional to the average bulk velocity of the material is the frequency corresponding to the peak of the power spectrum. Fig. 3.3(a) and Fig. 3.3(b) show a typical Doppler waveform and the power spectrum of this signal respectively. The standard deviation is approximately equal to (Hyltin et al., 1973)

$$\delta_{f_d} = \frac{\Delta f_d}{2} = \frac{v}{\lambda}\, \Delta\theta_2 \sin\theta \qquad (3.30)$$

where δ_{f_d} is the standard deviation of the instantaneous frequency f_{di}, Δf_d is the half power with of the spectrum, v is the velocity of the flow field, λ is the free space wavelength of the transmitting beam, $\Delta\theta_2$ is the two way 3dB beamwidth and θ is the viewing angle.

The area under the power spectrum curve gives the square of the RMS value of the Doppler signal, which is proportional to the density of the material. The area under the power spectrum is calculated using Simpson's formula as follows:

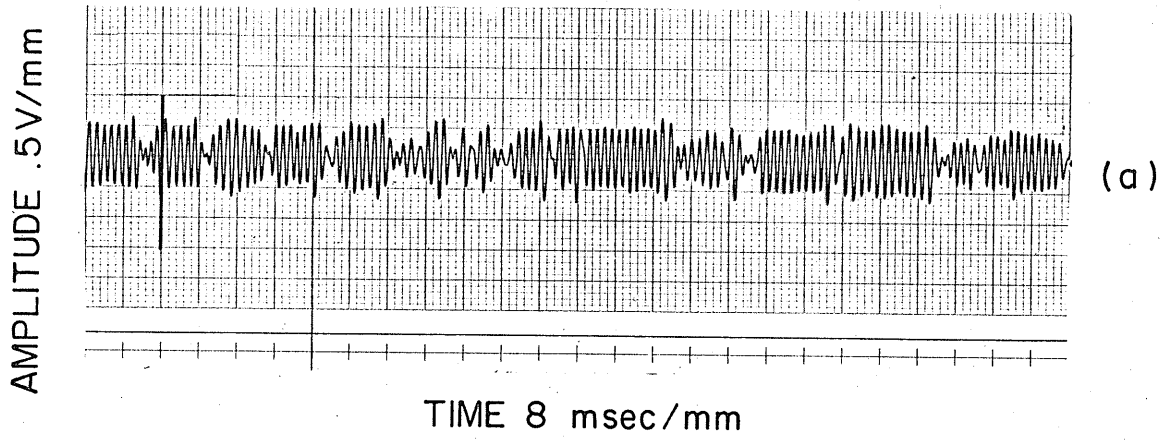

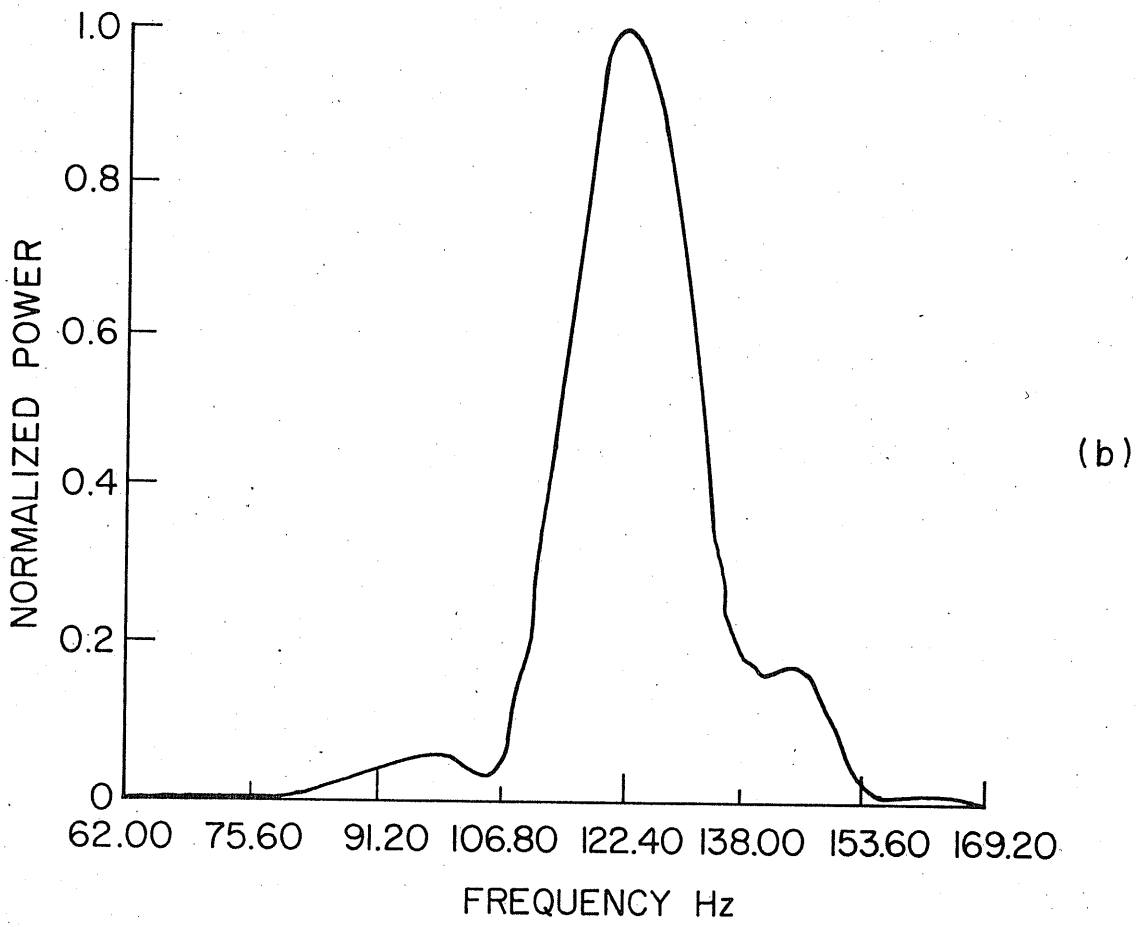

Figure 3.3 (a) Typical Doppler Waveform
(b) Typical Power Spectrum of the Doppler Signal

$$I(n) = [f(n=2) + 4f(n-1) + f(n)]/3 + I(n-2)$$

where,

f = the value of the data points

n = the constant time interval between consecutive data points (where n = 1, n + 2 = 2, ...)

CHAPTER IV

EXPERIMENTAL PROCEDURES

4.1 Introduction

Experiments were conducted with continuous bulk flow of wheat flowing through a section of a plastic pipe. The objective of the experiments was to verify the relationship between the average bulk density of grains and the RMS value of the Doppler radar output signal. Small metallic spheres were used to calibrate the Doppler radar. Three different flow fields were created during the course of experimentation, e.g. solid flow field, hollow flow field and elliptical flow field. The Doppler signal was processed on line by an anlog system and recorded for digital off line processing. Monostatic free space configuration was used throughout all the experiments.

4.2 Doppler Radar

A commerically available Doppler transceiver, model MA-86105 (Microwave Associates) operating at a frequency of 10.525 GHz and a standard waveguide horn, Narda 640, were used as the main sensing elements. The details of the different elements of the Doppler module and its operation have been described elsewhere (Hamid, 1975). A block diagram of a typical Doppler radar is given in Fig. 4.1.

4.3 Continuous Flow Experiments

In the free space configuration, a dielectric pyramidal box, lined with an absorbing mat, with the plastic pipe passing through the box and the Doppler radar module fixed at the other end of the box, was used throughout the experimentation in order to screen the interaction area

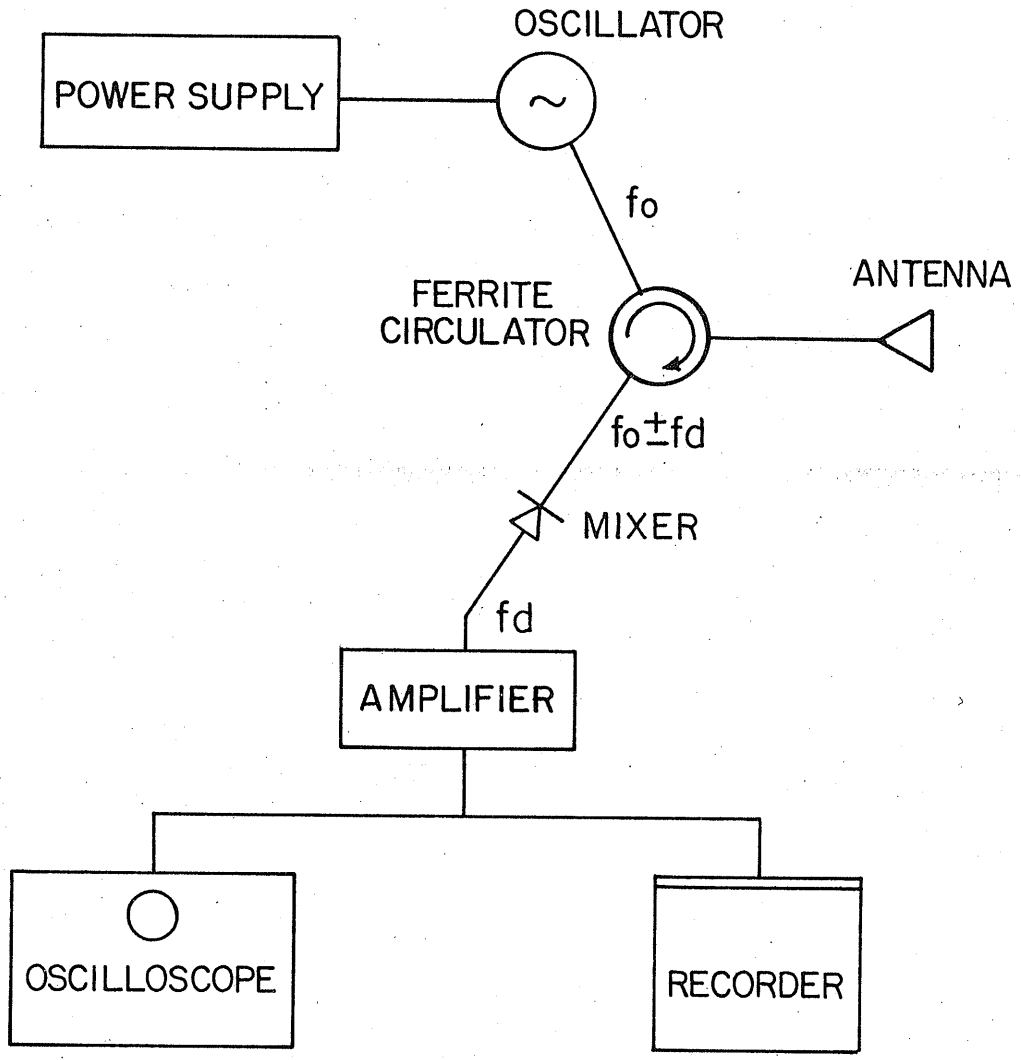

Figure 4.1 Block Diagram of a Typical Doppler Radar

from the surroundings and to minimize stray reflections. A general view of the experimental arrangement for a single scattering particle and for a continuous bulk flow is given in Fig. 4.2

In all the experiments, gravity flow was employed, in which the test material fell freely from a large hopper, through a section of plastic pipe into a collecting bucket located underneath. The material was recirculated by an auger conveyor.

The experiments were designed to measure the RMS value of the Doppler signal as a function of density of the material. The velocity of the material was measured at a fixed point in the flow field and kept at a constant value. The flow rate was varied by placing plastic orifices of different sizes on the top of the plastic pipe in order to vary the average bulk density. The moisture content and temperature of the material were kept constant at 12.5 percent (wet basis) and 70 F, respectively.

Weighing is a primary standard of flow measurement, and therefore, a direct weighing technique was used to determine the mass flow rate for the purpose of calculating the average density of the test material falling freely through the pipe.

A viewing angle of 42.5° was used in all experiments because it was found optimum for the measurement of the velocity of the target (Hamid, 1975).

4.4 Analog Signal Processing Arrangement - On Line

In the analog signal processing arrangement, the Doppler module was supplied from a power supply (HP 6220 B). The output signal from the module was amplified by a pass-band amplifier (PAR 113) and further displayed on the screen of a storage oscilloscope (Tektronix 564 B). A true RMS voltmeter (HP 3400 A) was incorporated for measurement of the RMS value of the Doppler radar signal. A strip chart recorder (Clevite Brush Mark 220)

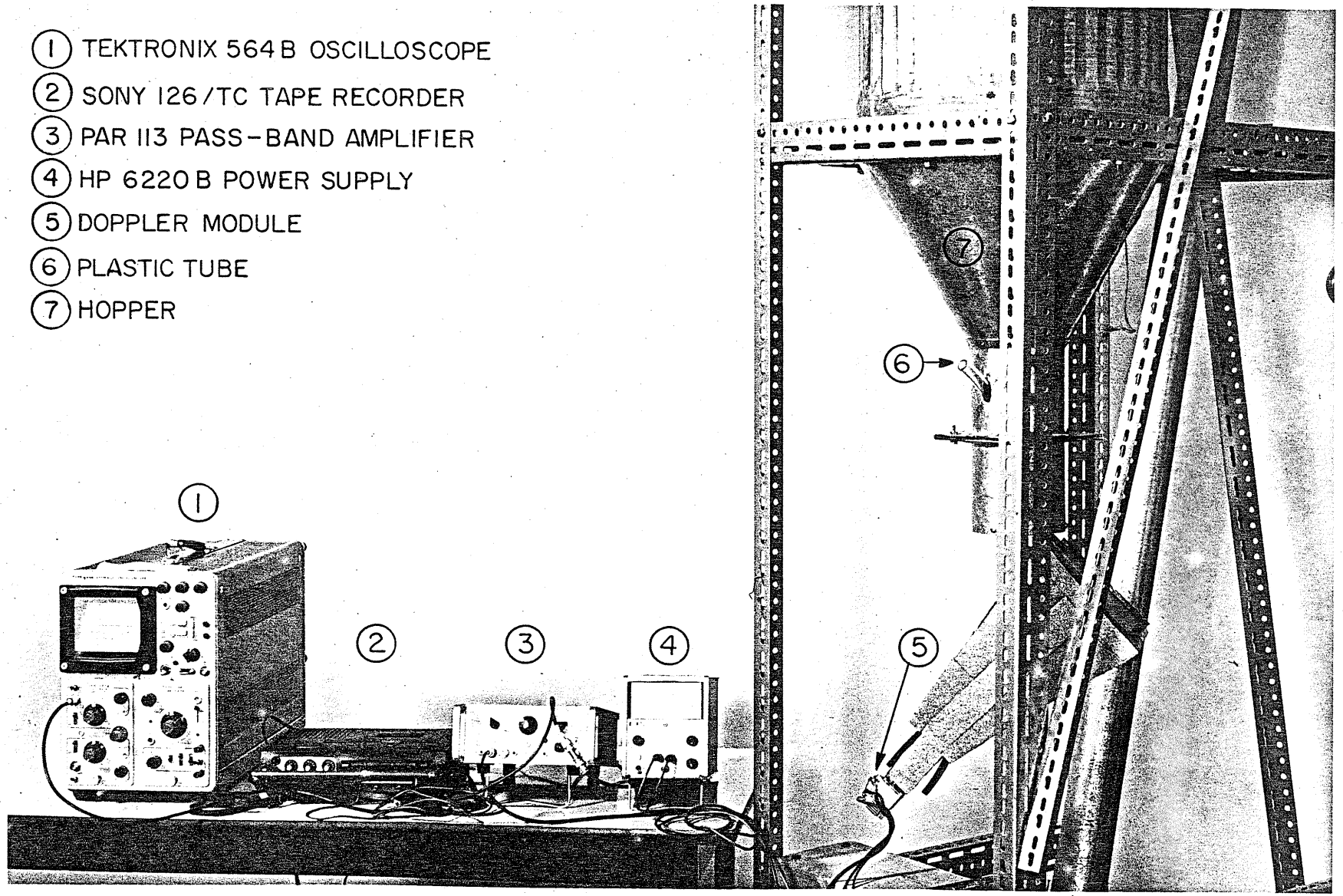

Figure 4.2 General View of the Experimental Arrangement for Single Scattering Particle and Continuous Bulk Flow

was used for continuous recording of the DC output signal from the true RMS voltmeter which was proportional to the RMS value of the Doppler signal. Averaging times of 1,3, and 5 seconds were used. Capacitors of 1000, 3000, and 5000 μF were connected in parallel to the input of the strip chart recorder. A general view of the analog signal processing arrangment is shown in Fig. 4.3.

4.5 Digital Signal Processing Arrangement - Off Line

In the digital signal processing system, the Doppler signal was amplified by a pass-band amplifier (PAR 113) and displayed on a storage oscilloscope (Tektronix 564 B). The signal was continuously recorded on magnetic tape by a tape recorder (Sony TC-126) for further processing by a digital computer. The signal was then fed through a pass-band amplifier to a digital computer (Digital Equipment Co. PDP-11/40) through Lab Peripheral System LPS-11. The signal was digitized at the rate of 2000 points per second. A sample of the digitized Doppler signal displayed on the screen of the computer CRT is shown in Fig. 4.4. A general view and a schematic diagram of the digital signal processing arrangement are given in Fig. 4.5 and Fig. 4.6, respectively.

The PDP-11 computer is interfaced with the LPS-11 Lab Peripheral System. The system houses a 12-bit A/D converter, a programmable real time clock, a display unit and a 16-bit digital I/O option. A schematic diagram of the LPS is shown in Fig. 4.7.

The information and commands were communicated to the computer by teletype. The results of the computations were displayed on the screen of the display unit (LPSVC). The A/D converter (LPSAD-12) sampled the analog data (Doppler signal) at specified rates and stored the equivalent digital values for subsequent processing. A schematic diagram of LPSAD-12 is shown in Fig. 4.8.

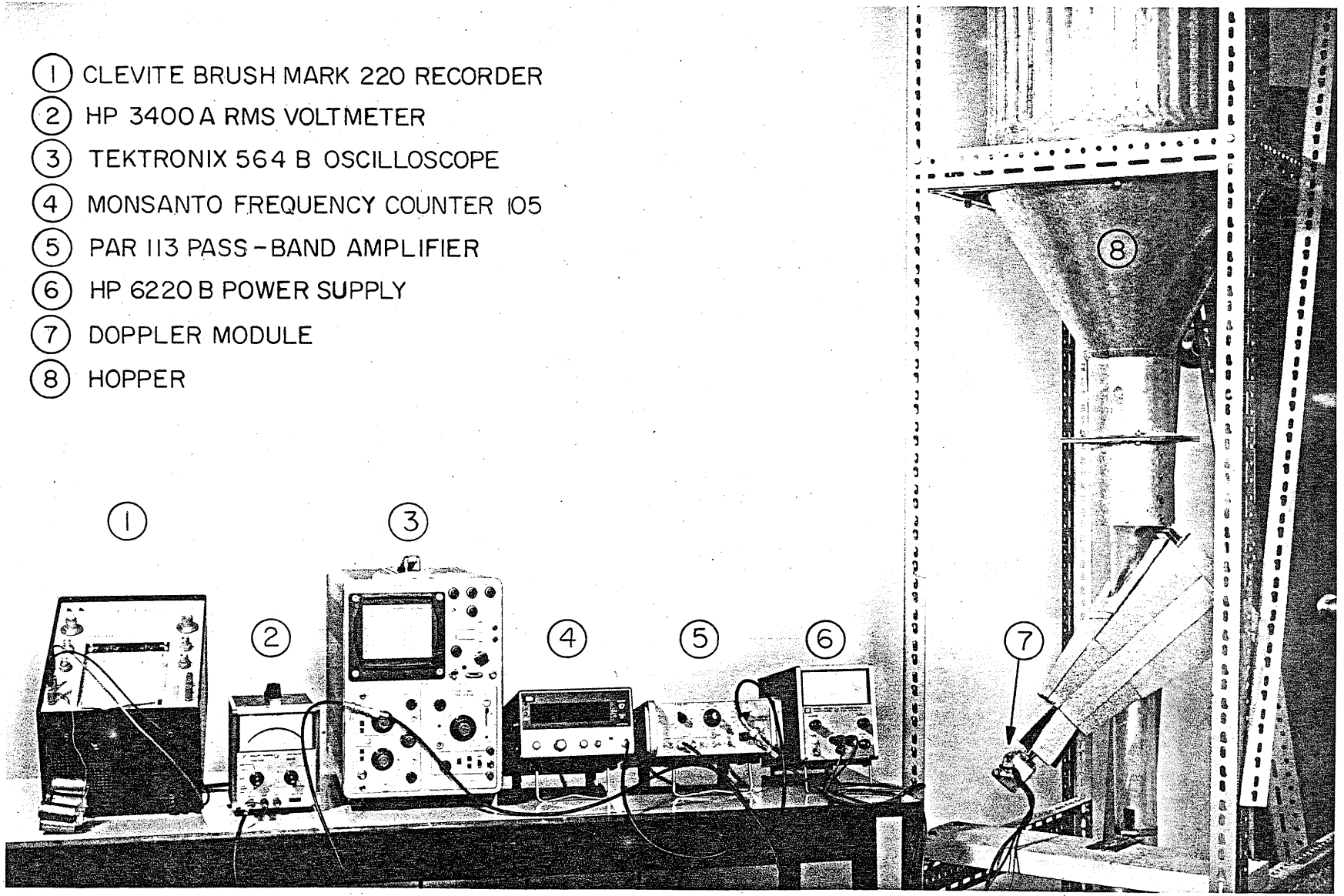

Figure 4.3 General View of the Analog Signal Processing Arrangement

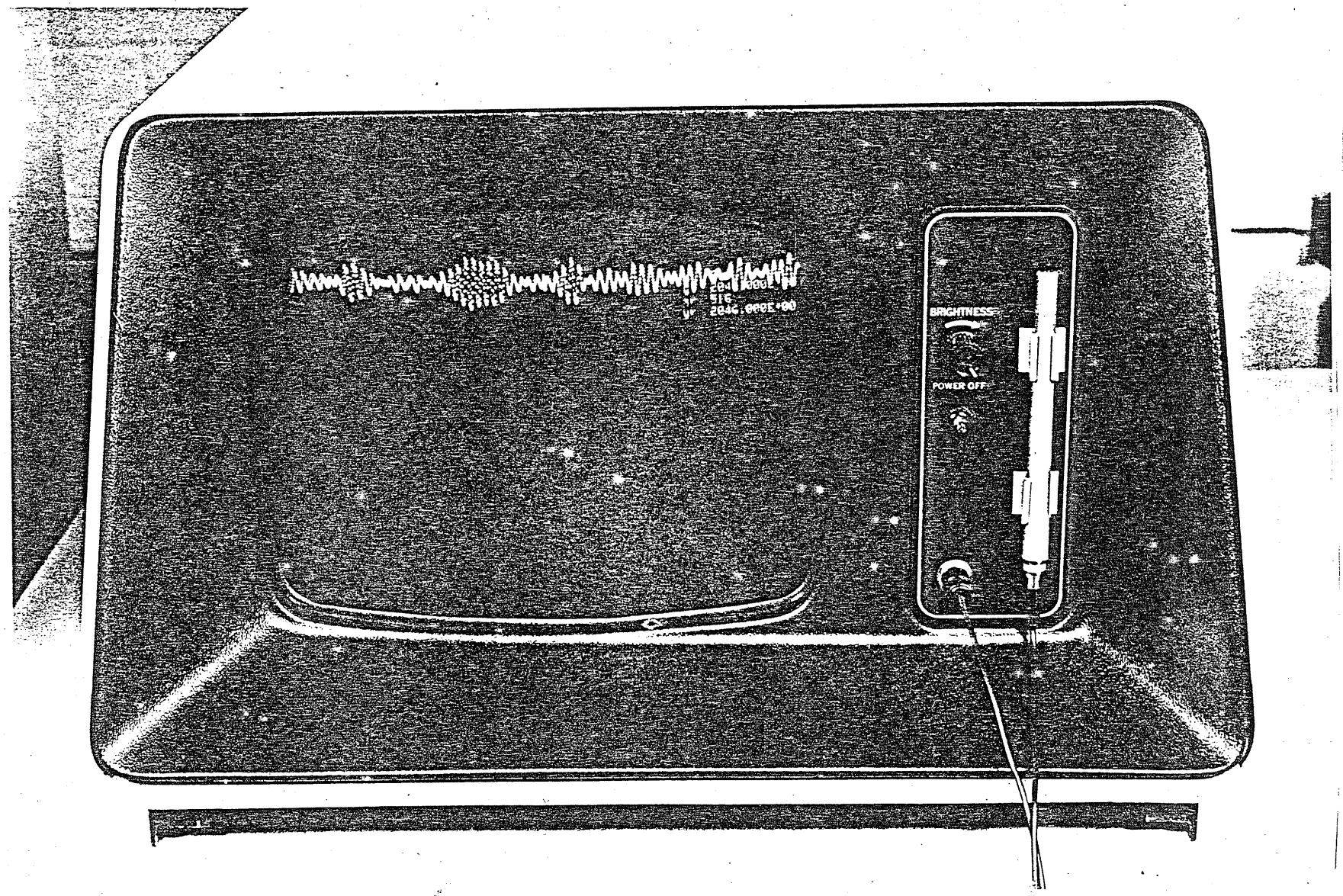

Figure 4.4 A Sample of the Digitized Doppler Signal Displayed on the Screen of the Computer.

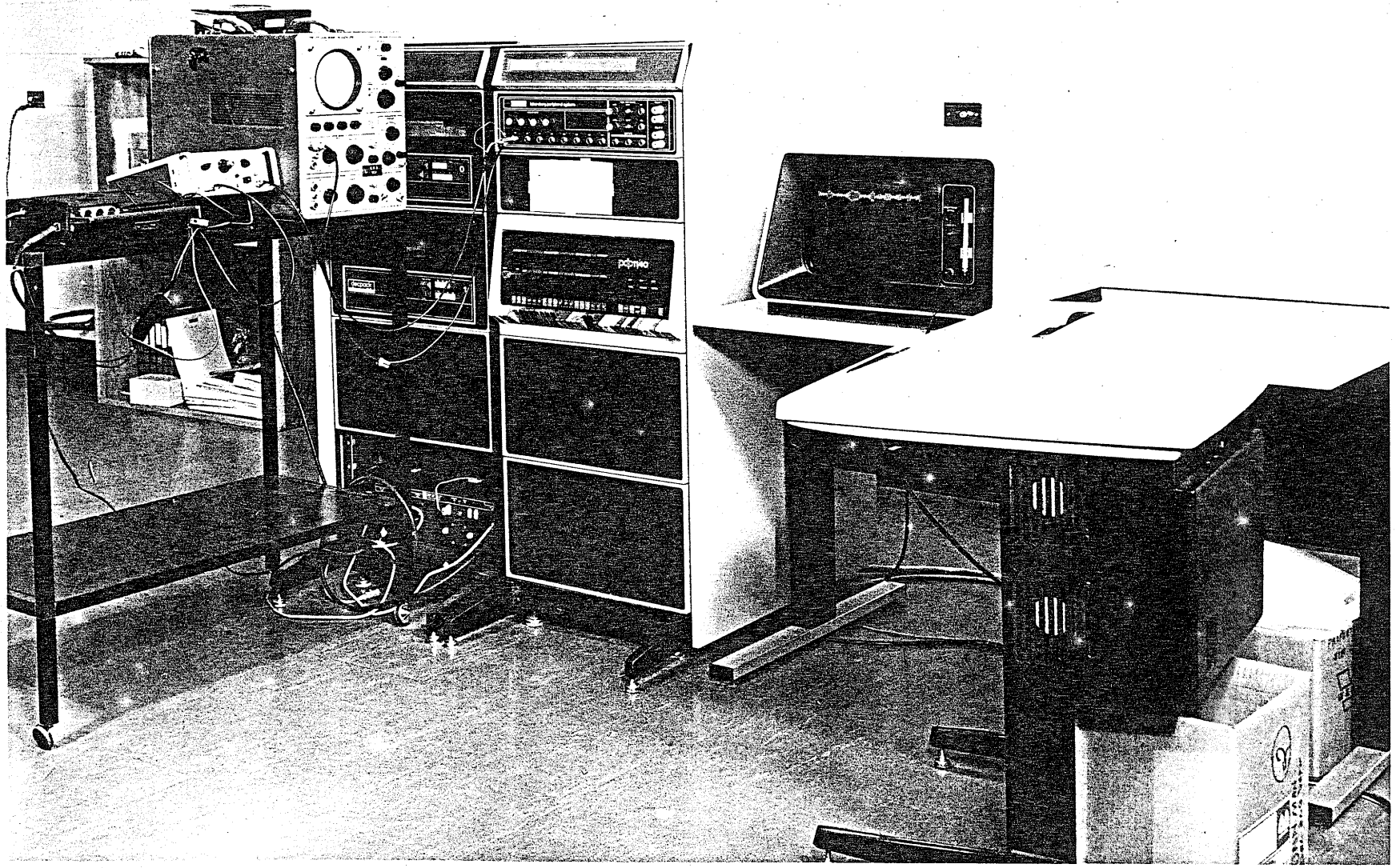

Figure 4.5 General View of the Digital Signal Processing Arrangement

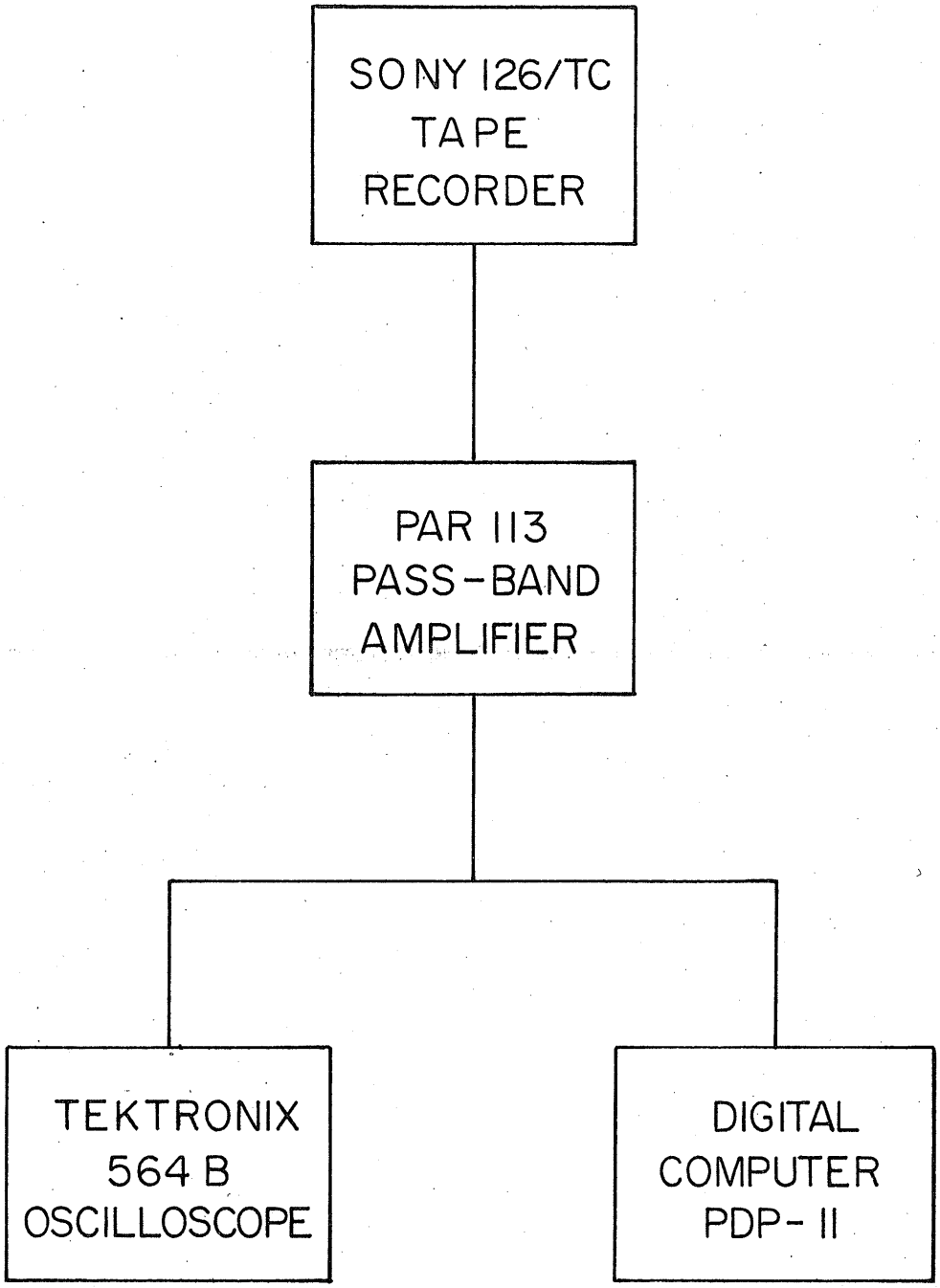

Figure 4.6 Schematic Diagram of the Digital Signal Processing Arrangement

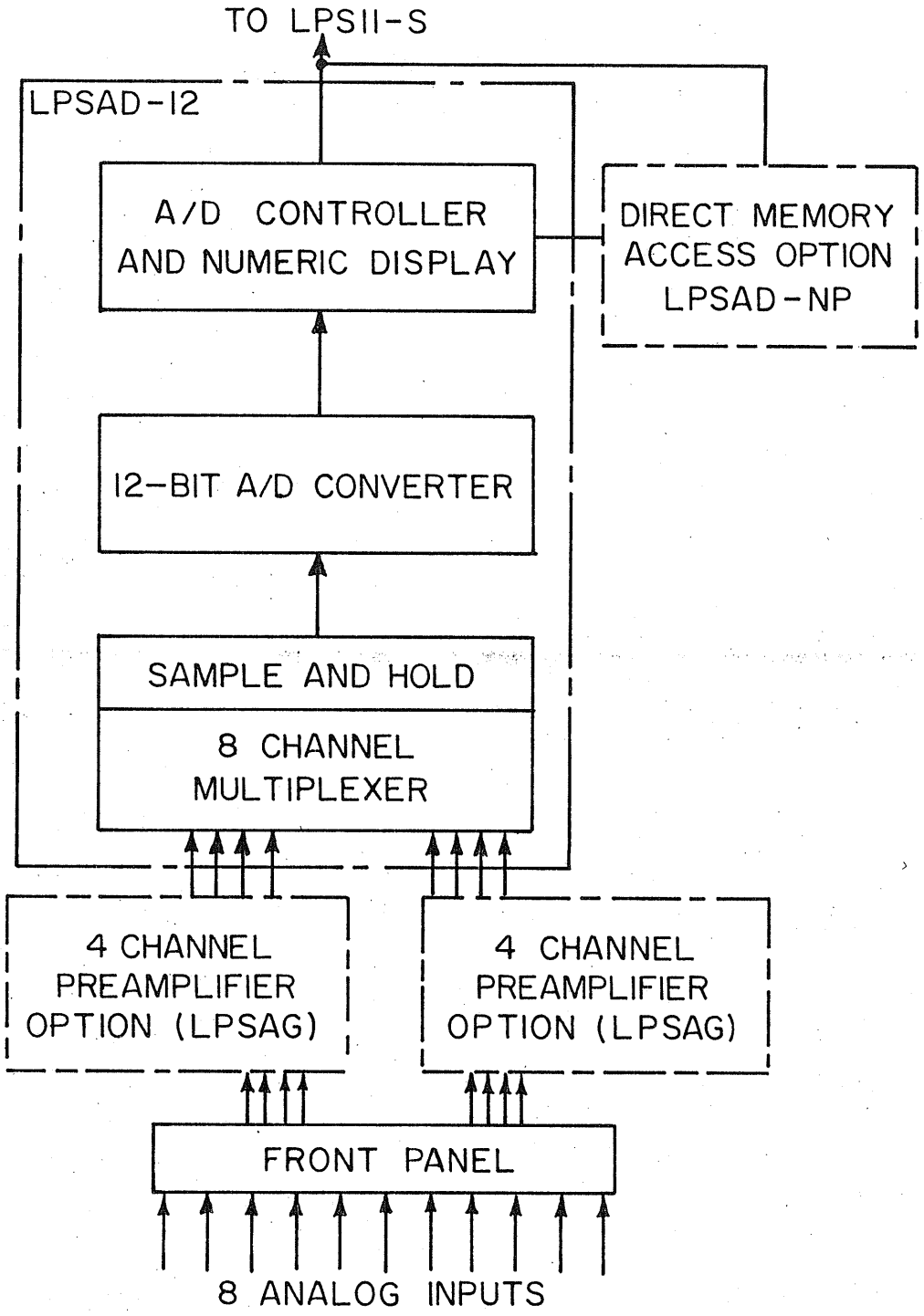

Figure 4.7 Schematic Diagram of the Laboratory Peripheral System (LPS-11)

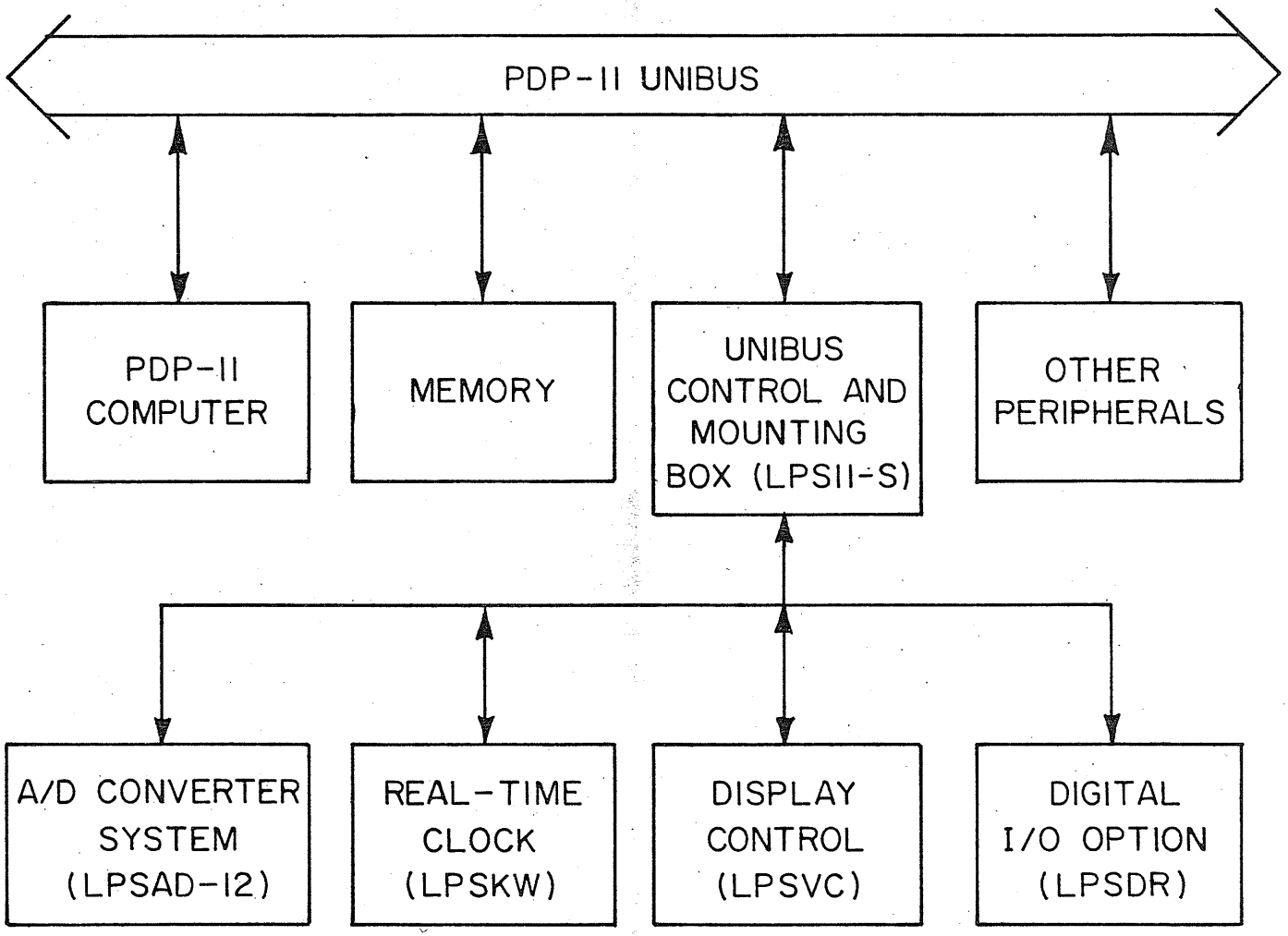

Figure 4.8 Schematic Diagram of A/D Converter System (LPSAD-12)

The fast Fourier transform and the power spectrum were calculated by the computer by using the software package of the computer (SPARTA). The power spectrum was displayed on the screen and the RMS value of the Doppler signal and the mean Doppler frequency were calculated from the power spectrum, The Doppler signal from metallic calibrating spheres was also analysed by a digital computer.

4.6 Experiments for Average Bulk Density Measurement of Wheat

In continuous flow experiments, the average bulk density of wheat was measured by measuring the mass flow rate by a direct weighing and timing technique. The velocity of the grains was measured at a fixed point in the flow field and kept at a constant value. The area of the flow field was assumed to be the same as that of the orifice.

4.7 Procedure of Creating Flow

Four different flow fields were created during the period of experimentation. The four different flows employed were, single scattering particles (metallic spheres), continuous solid bulk flow, hollow flow and elliptical flow.

For single scattering particles, metallic spheres of different sizes were used. A small hole was made in the metallic pipe, welded to the bottom of the hopper, to accomodate a flexible plastic tube for dropping the metal spheres in the centre of the plastic pipe. A general view showing the arrangement for single scattering particle is shown in Fig. 4.2. Solid bulk flow was obtained by plastic orifices of different sizes in order to have different bulk densities at the centre of the pipe. The hollow flow field was created by attaching circular cones of different sizes in the centre of the orifices. Elliptical flow was the result of an elliptical orifice placed at the top of the plastic pipe.

4.8 Signal Recording Unit

A tape recorder (Sony TC-126) was used for recording the signal on magnetic tape for further processing by a digital computer (DEC PDP-11/40). Frequency response of this recorder was 50 - 10,000 Hz for standard cassette and 50 - 13,000 Hz for chromium dioxide cassettes. This tape recorder has two input channels, microphone inputs and line inputs. The signal to noise ratio for the tape recorder was 45 dB.

CHAPTER V

RESULTS AND DISCUSSION

5.1 Introduction

Following the procedure outlined in Chapter IV, metal spheres of various sizes were used for calibration of the radar system. The RCS of columns of wheat falling in a plastic pipe were then measured by measuring the RMS values of the Doppler signal. The average bulk densities of the falling columns were determined for different mass flow rates. The experimental uncertainties in the measurements of the average bulk density, the average mass flow rate, and the corresponding RCS were analysed. Doppler signals were processed by two different techniques: an analog, (on line) and a digital (off line). Various experimental results of the RCS as a function of the average bulk density of granular material are presented. Theoretical results are compared with the experimental data.

5.2 Calibration of the Radar System

Metallic spheres of different sizes, with RCS calculated theoretically, were used to calibrate the radar system. This method of comparison is quite common. In this method the power scattered by the object under test is compared with the power scattered by a standard located in the same position as the object. A metallic sphere is commonly used as a RCS standard.

The RCS of most of the particulate solids of interest falls in the Rayleigh region (for the selected frequency range) and, therefore, small metallic spheres were used. Theoretically, the monostatic scattering cross-section of a metal sphere in the Rayleigh region is given by eq. 3.9.

Experimentally, the RCS of a sphere was determined by a digital computer. The signal was digitized at a rate of 2000 points per second. A general view of the digitized Doppler signal fed to the computer for a single scattering particle (metal sphere) is shown in Fig. 5.1. Fig. 5.2 depicts a typical power spectrum of the Doppler signal obtained by digital processing of the output signal from the Doppler radar sensor shown in Fig. 5.1. The area under the power spectrum curve was determined, and was related to the RCS of metallic sphere calculated theoretically.

Table 5.1 gives a comparison of theoretical and experimental values of the RCS of various metallic spheres. The experimental values are in good agreement with the theoretical ones.

TABLE 5.1

Comparison of Experimental and Theoretical Values of the RCS of Various Metal Spheres

Diameter (m) $\pm 2.5 \times 10^{-5}$ m	Theoretical RCS $\times 10^{-4}$ m^2	Uncertainty in Theoretical RCS ($\pm$%)	Experimental σ/σ_o^*	Theoretical σ/σ_o^*	Difference (%)
.0078	2.350	1.702	7.34	7.339	0.013
.0064	0.720	1.805	2.250	2.388	5.77
.0056	0.320	3.125	-----	-----	-----
.0048	0.128	3.450	0.400	0.372	7.00
.0040	0.042	4.760	0.131	0.130	0.760

*The RCS of a .0056 m sphere

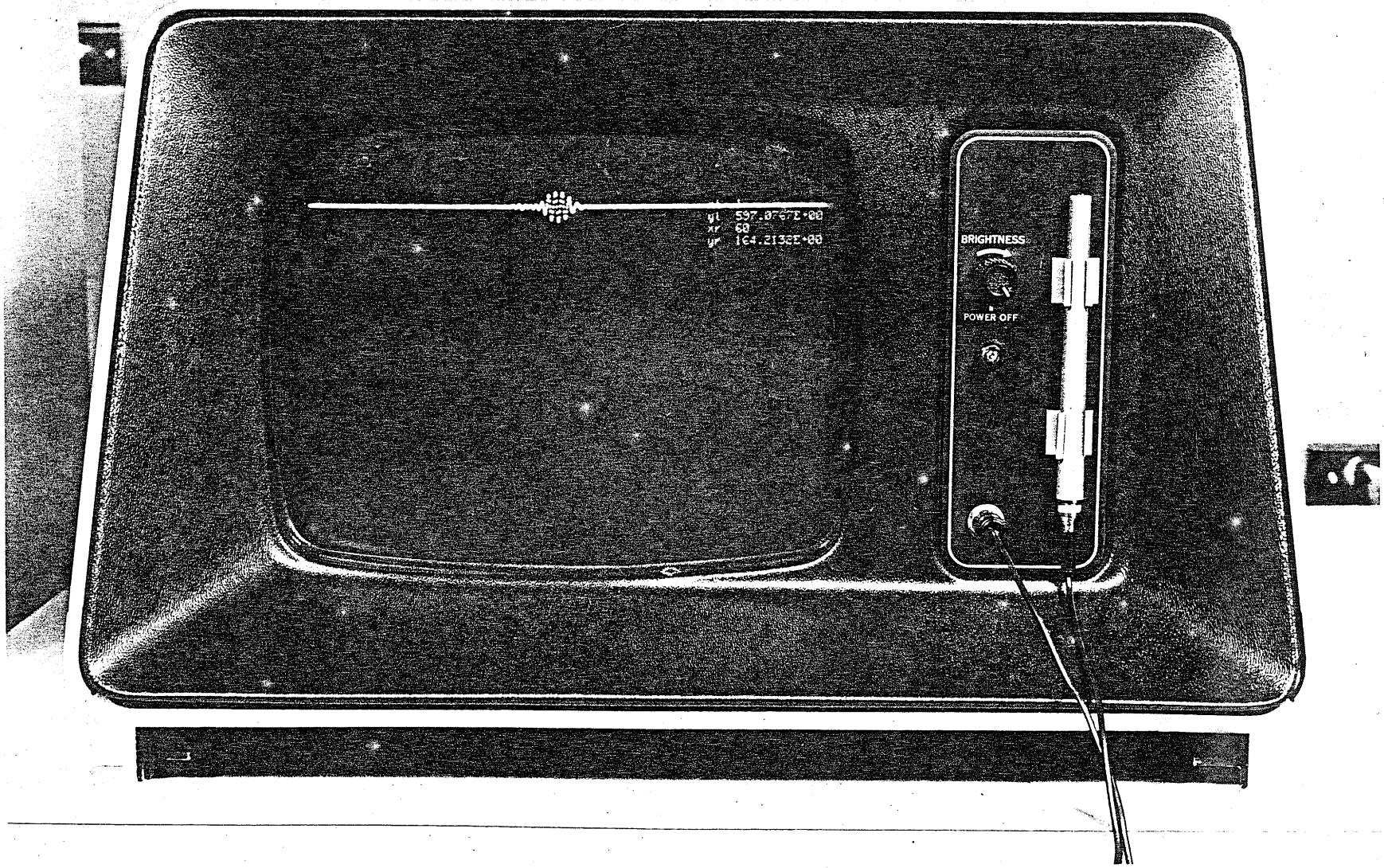

Figure 5.1 General View of the Digitized Doppler Signal Fed to the Computer for a Single Scattering Particle (Metal Sphere)

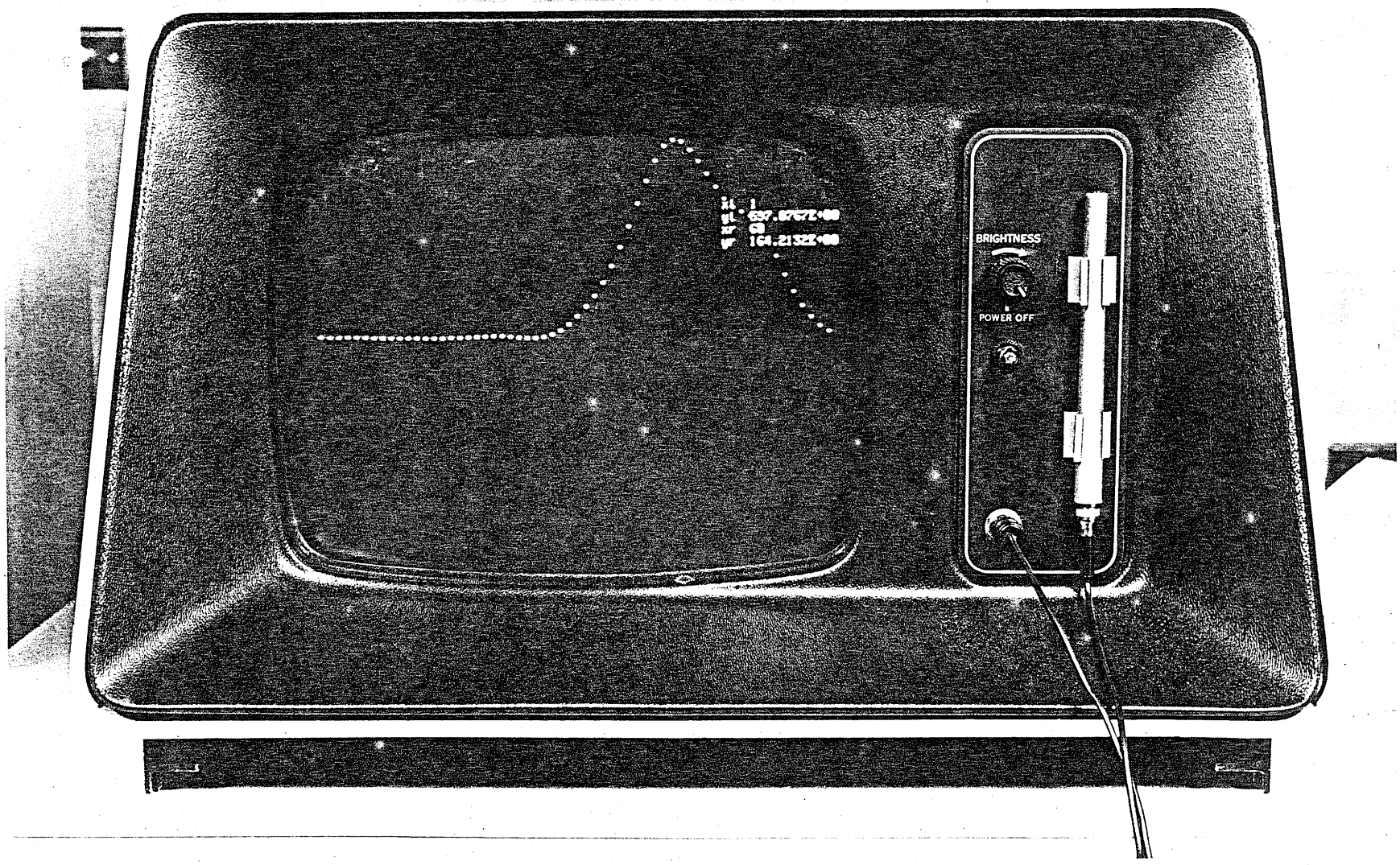

Figure 5.2 Typical Power Spectrum of the Doppler Signal Obtained by Digital Processing of the Output Signal from the Doppler Radar Sensors Shown in Fig. 5.1

5.3 Calibration of the Flow Field

A direct weighing and timing technique was employed in order to determine the average mass flow rate of wheat in the continuous flow experiments. The average bulk density of the flowing wheat was calculated from the following eq. 3.1

$$M_{av} = A_{av} \times D_{av} \times V_{av}$$

where, M_{av} is the average mass flow rate in Kg/sec, A_{av} is the average area of cross-section of the illuminated flow field in m^2, D_{av} is the average bulk density in Kg/m^3, and V_{av} is the average velocity of grains in m/sec.

The average velocity of the flowing material, V_{av}, was calculated from the mean Doppler frequency measured by a frequency counter (Monsanto Model 105A). A schematic diagram and a general view of the frequency counting arrangement are given in Fig. 5.3 and Fig. 5.4, respectively. The mean Doppler frequency was also determined from the power spectrum of the Doppler signal. The results will be discussed in 5.5.4(b). The Doppler frequency and the velocity of target are related as follows (Skolnik, 1962):

$$f_d = \frac{2f_o}{c} v \cos \theta \qquad (5.1)$$

and hence

$$v = \frac{c}{2f_o} \cdot f_d/\cos \theta \qquad (5.2)$$

where v is the velocity of moving material in m/s, f_d is the Doppler frequency in Hz, f_o is the frequency of transmitted beam in Hz, c is the velocity of propagation of the electromagnetic waves in m/s, and θ is the viewing angle in degrees.

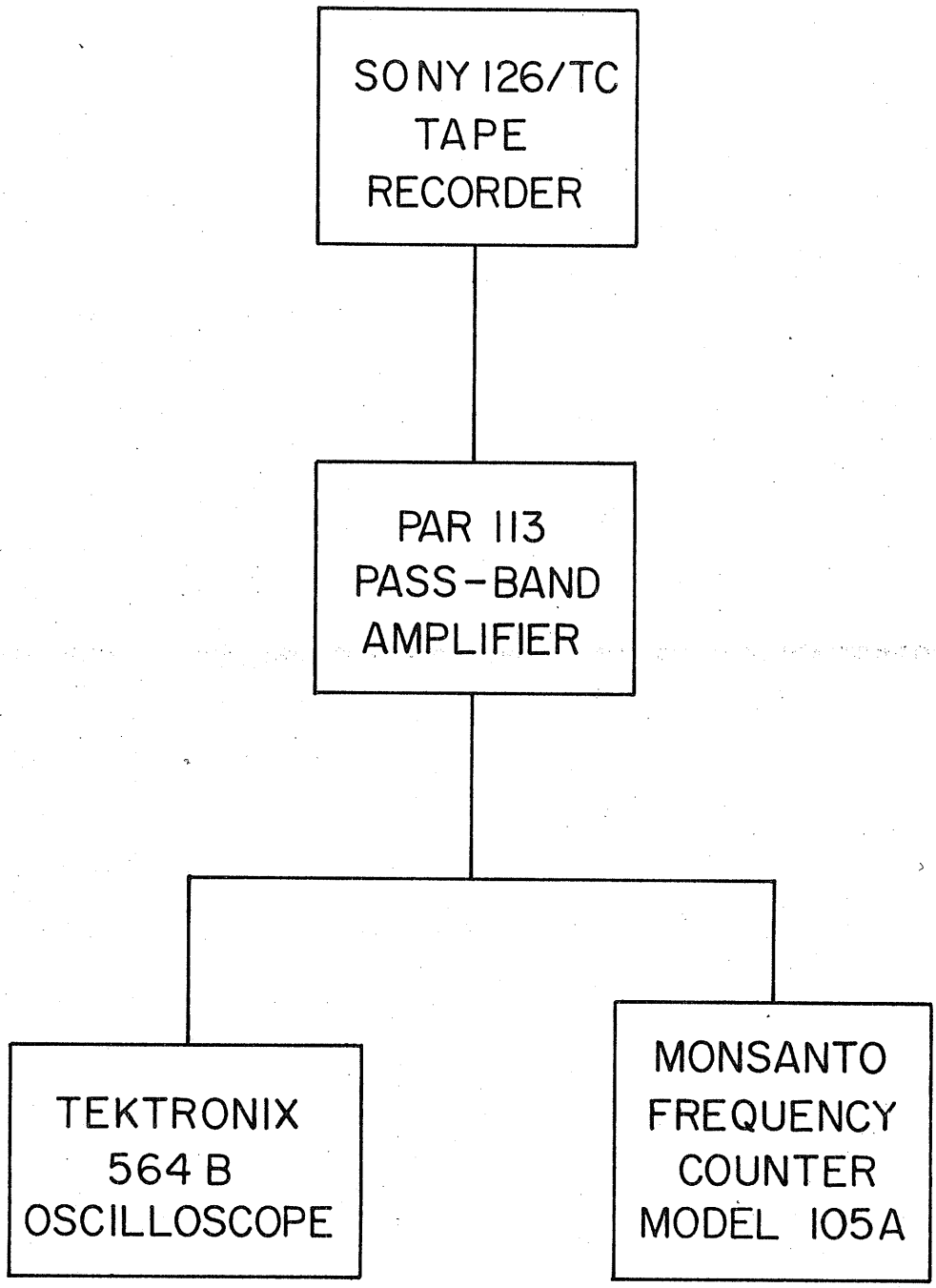

Figure 5.3 Schematic Diagram of the Frequency Counting Arrangement

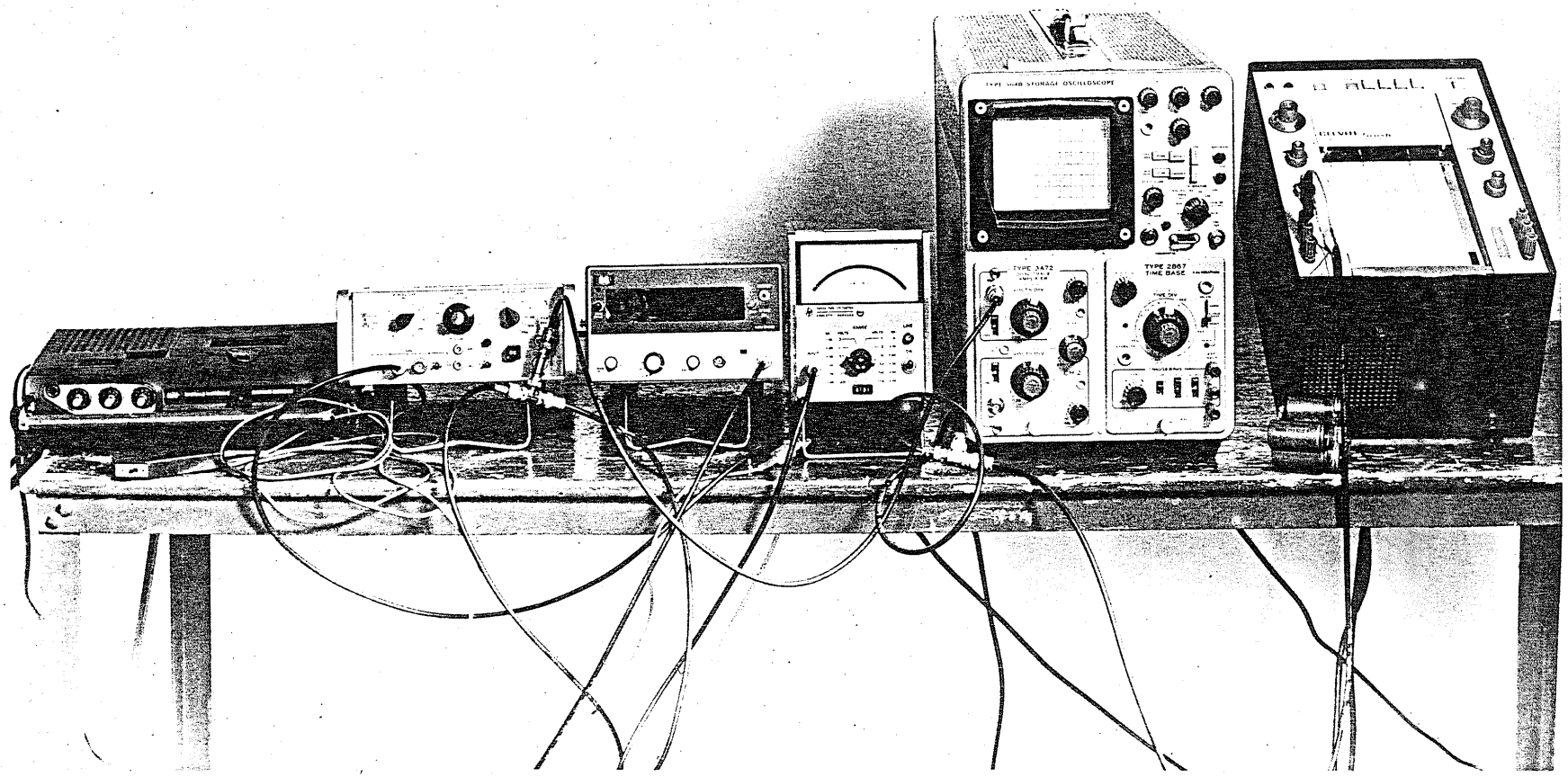

Figure 5.4 General View of the Frequency Counting Arrangement

In the experiments reported here an averaging time of 3 sec was used to calculate the average Doppler frequency. This proved to be necessary because the Doppler signal scattered by the bulk flow of wheat is not steady in time. The free falling flow of wheat consists of bunches rather than a continuous flow. The particles neither move in one direction nor have they the same velocities. The particles have random movements, i.e., spinning, bouncing, to and fro motions etc., and have different scattering properties which make the Doppler signal complex. Similar results have also been reported (Marshall and Hitschfeld, 1953) for scattering and attenuation of meteorogical particles. It was shown that an instantaneous observation of the received signal gives very little information about the precipitation, and the signal at any given range has to be averaged until a large number of independent returns have been received.

Velocity measurements of granular materials by Doppler radar have been done and reported elsewhere (Hamid, 1975). It was found that the frequencies of the Doppler signal from single scattering particles were spread over a finite bandwidth, but the mean frequency of the Doppler spectrum gave accurate values of velocities for a given viewing angle. A simplified diagram showing the reference point for velocity measurements in the flow field is shown in Fig. 5.5.

The cross-section area of the flow field was assumed to be the same as that of the orifice through which the material fell in the centre of the plastic pipe. Some small dispersion occured as the material passed through the orifice and moved in the pipe. The resulting uncertainty in measurement of the average bulk density due to the change in the cross-section area of the flow field will be discussed in 5.4.1.

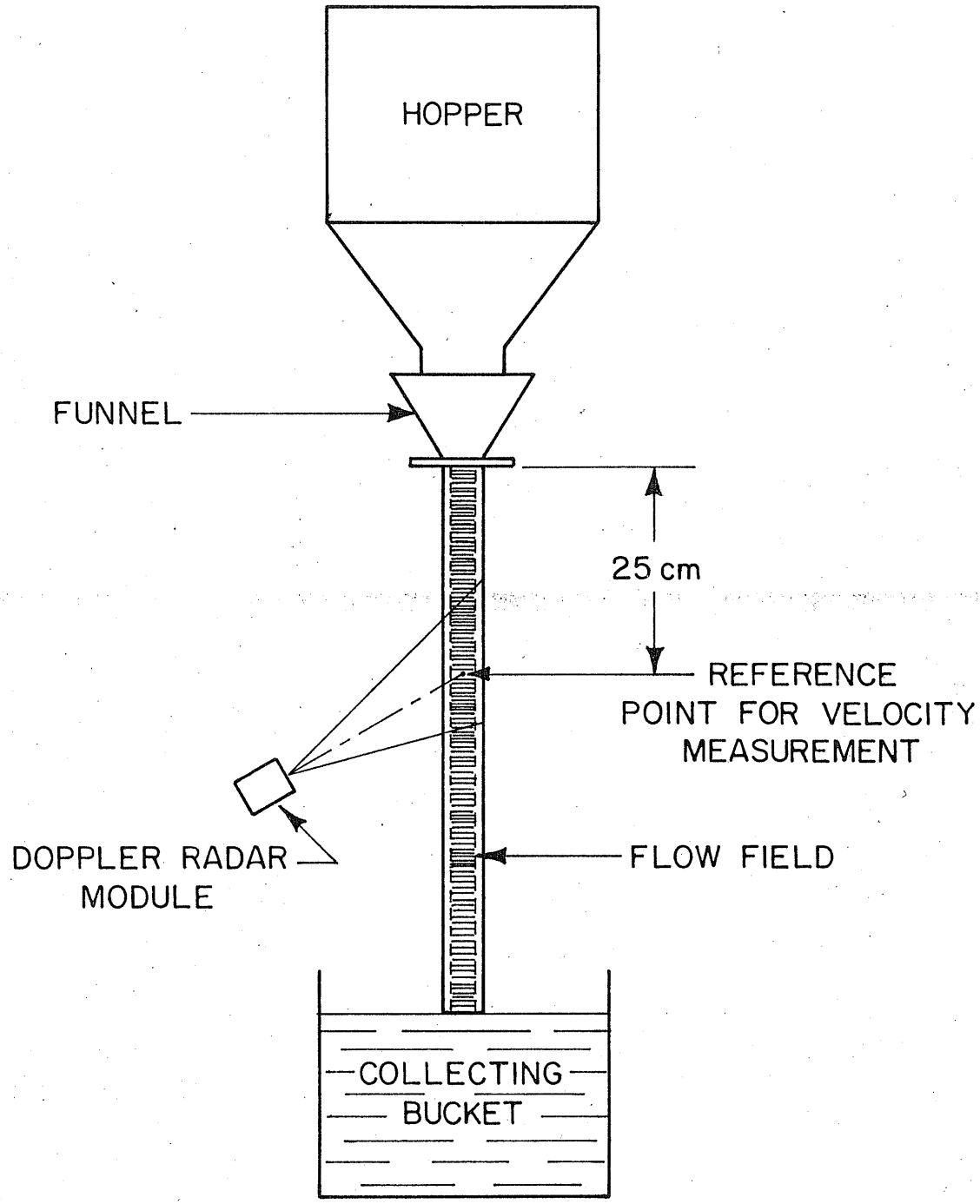

Figure 5.5 Diagram Showing the Reference Point for Velocity Measurements in the Flow Field

Substituting eq. 5.2 into eq. 3.1 and rearranging

$$D_{av} = \frac{M_{av}}{A_{av} \cdot c \cdot f_d} \cdot 2f_o \cdot \cos\theta \qquad (5.3)$$

where symbols carry the same meaning as in eqs. 3.1 and 5.2. The average bulk densities calculated for different mass flow rates of wheat are listed in Table 5.2.

5.4 Experimental Uncertainty

The uncertainty in caculating the average bulk density of wheat from eq. 5.3 is caused by three uncertainties, namely in measurement of the cross-section area of the flow field, in weighing of the granular material, and in recording the time of flow i.e., starting and stopping the stop watch synchronously with the flow. The other parameter creating uncertainty in density determination is the velocity of particulate solids which has been analysed and reported elsewhere (Hamid, 1975).

TABLE 5.2

Average Bulk Densities of Wheat at Different Flow Rates, Average Velocity = 2.2 m/sec

Diameter of the Flow Field (m)	Flow Rate (kg/sec)	Average Bulk Density (kg/m^3)
0.05	.534	125.3
0.04	.310	113.3
0.035	.209	98.7
0.03	.134	88.0
0.025	.074	67.9

The uncertainty in determining the RCS comes from uncertainties in measurement of the diameter of a calibrating sphere and in measurement of the RMS value of the Doppler signal by a RMS voltmeter. Errors in calculating the RMS value of the Doppler signal by a computer are very small and, therefore, can be neglected.

A method of estimating uncertainty in experimental results has been suggested (Kline and McClintock, 1953) in the following form.

If S is a given function of independent variables x_1, x_2, x_3, ..., x_n .

Then

$$W_S = [(\frac{\partial S}{x_1} w_1)^2 + (\frac{\partial S}{x_2} w_2)^2 + \ldots + (\frac{\partial S}{x_n} w_n)^2]^{1/2} \tag{5.4}$$

where W_S is the uncertainty in the result S, w_1, w_2, ... and w_n are the uncertainties in the independent variables.

5.4.1 Density

The average mass flow rate of the granular material is given by eq. 3.1

$$M_{av} = A_{av} \times D_{av} \times V_{av} \tag{5.5}$$

where notations bear the same meaning as in eq. 3.1 . Further

$$D_{av} = \frac{M_{av}}{A_{av} \times V_{av}} \tag{5.6}$$

while

$$M_{av} = \frac{W}{T} \tag{5.7}$$

where W is the weight of the material in kg, and T is the time period of the flow in seconds.

Substituting eq. 5.7 into eq. 5.6

$$D_{av} = \frac{W}{A_{av} \times V_{av} \times T} \tag{5.8}$$

where symbols carry the same meaning as in eqs. 5.6 and 5.7.

The uncertainty in the calculation of the density can be found by differentiating eq. 5.8 with respect to independent variables, W, T, V, and A as follows:

$$\frac{\partial D_{av}}{\partial W} = \frac{1}{A_{av} \cdot V_{av} \cdot T}$$

$$\frac{\partial D_{av}}{\partial T} = - \frac{W}{A_{av} \cdot V_{av} \cdot T^2}$$

$$\frac{\partial D_{av}}{\partial V_{av}} = - \frac{W}{A_{av} \cdot V_{av}^2 \cdot T}$$

$$\frac{\partial D_{av}}{\partial A_{av}} = - \frac{W}{A_{av}^2 \cdot V_{av} \cdot T}$$

Hence

$$W_{D_{av}} = \left[\left(\frac{\partial D_{av}}{\partial W} w_1\right)^2 + \left(\frac{\partial D_{av}}{\partial T} w_2\right)^2 + \left(\frac{\partial D_{av}}{\partial V_{av}} w_3\right)^2 + \left(\frac{\partial D_{av}}{\partial A_{av}} w_4\right)^2\right]^{1/2} \tag{5.9}$$

where, $W_{D_{av}}$ is the uncertainty in the average bulk density of particulate solids, w_1, w_2, w_3, and w_4 are the uncertainties in the weight of material, time period of the flow, measurement of the velocity of particulate solids and the cross-section area of the flow field, respectively.

The experimental uncertainty in measurement of the average bulk density of granular materials calculated from eq. 5.9 is given in Table 5.3 for three bulk densities.

TABLE 5.3

Uncertainties in Measurement of the

Average Bulk Density of Wheat, Average Bulk Velocity = 2.2 m/sec

Diameter of the Flow Field Column (m)	Average Bulk Density (kg/m^3)	Uncertainty (%)
0.050	125.3	5.6
0.035	98.7	5.7
0.030	88.0	6.0

5.4.2 Radar Cross-section

If the diameter of the sphere is $d + \Delta d$, instead of d, the RCS is given by

$$\sigma = \frac{4}{\pi} K^4 \left[\frac{4}{3} \pi \left(\frac{d + \Delta d}{2}\right)^3\right]^2 F^2 \qquad (5.10)$$

compared with

$$\sigma = \frac{4}{\pi} K^4 \left[\frac{4}{3} \pi \left(\frac{d}{2}\right)^3\right]^2 F^2$$

for the nominal diameter d, where d is the diameter of the sphere and other symbols are same as in eq. 3.9. Thus for the diameter of 0.0056m, the uncertainty of $\pm 2.5 \times 10^{-5}$ m causes an uncertainty in σ of 3.1 percent. If the RMS value of the Doppler signal is measured with an uncertainty of 1 percent, the uncertainty in the RCS of column of wheat is 3.25 percent.

5.5 Continuous Flow Experiments

5.5.1 Multiple Scattering

The continuous flow of particulate solids involves a problem of multiple scattering. The Doppler signal results from contributions of signals scattered by a large number of particles. Each scattering particle has, in general, different scattering properties. Mutual interactions between the scatterers also affect the resultant signal. Fluctuations of the radar cross-section with the viewing aspect add to the complexity of the problem. Furthermore, particles move neither in one direction nor at the same velocity. Random movementsof particles, along with the factors discussed above, result in a complex waveform of the Doppler signal.

5.5.2 Averaging Technique

The discussion in the previous section leads to the conclusion that the instantaneous Doppler signal contains little information about the average flow rate of granular materials. However, long time averages (a few seconds) of the instantaneous Doppler signals were found to be proportional to average bulk densities. Marshall and Hitschfield (1953) have demonstrated the necessity of averaging of instantaneous signals scattered by meteorogical particles in order to extract the desired information. The same averaging concept was used by Arts and Roevros (1971) to measure blood flow rate by ultrasonic means.

5.5.3 Analog Signal Processing Technique

(a) Circular Cross-section Flow Field - The experiments were performed with wheat falling freely under gravity through plastic orifices of different sizes, placed at the top of a plastic pipe, in order to obtain

different flow rates and hence different bulk densities. The objective of the experiments was to find a relationship between the average RMS value of the Doppler signal and hence RCS and the average density of the flow field. Figs. 5.6(a), (b), and (c) show the typical recordings of RMS value of the Doppler signal averaged for 1 sec, 3 sec, and 5 sec.

Inspection of Figs. 5.6(a), (b), and (c) reveals that 1 sec averaging time is insufficient to obtain reliable information about the flow field. However, 3 sec and 5 sec averaging time was found to be sufficient to extract quantitative information about average flow rates of particulate solids. The RMS value of the Doppler signal for 1 sec averaging time varied $\pm$ 9 percent around the mean value obtained for 5 sec averaging time, while it varied only $\pm$ 1 percent for 3 sec averaging time. As the difference between 3 sec and 5 sec averaging for the Doppler signal output is small, therefore, 3 sec averaging time was considered to be appropriate for retrieving meaningful information about the flow field.

The RMS values of the Doppler signal recorded at different flow rates having different bulk densities, were used to calculate RCS of columns of wheat. The RCS of the column of wheat with bulk density of 125.3 kg/m^3 computed by a digital computer was used as a reference, e.g., it is common in Figs. 5.7(a) and (b). Fig. 5.7(a) shows the RCS as a function of the average bulk density of wheat. It is evident from this figure that the RCS varies linearly with the bulk density. The RMS deviation of the experimental points from the straight line calculated by least square analysis is equal to 1.2 percent.

(b) Ring Cross-section Flow Field - Experiments were also conducted with the flow of wheat with a ring shape cross-section having a hollow space in the centre of the flow field. The objective of this test was to

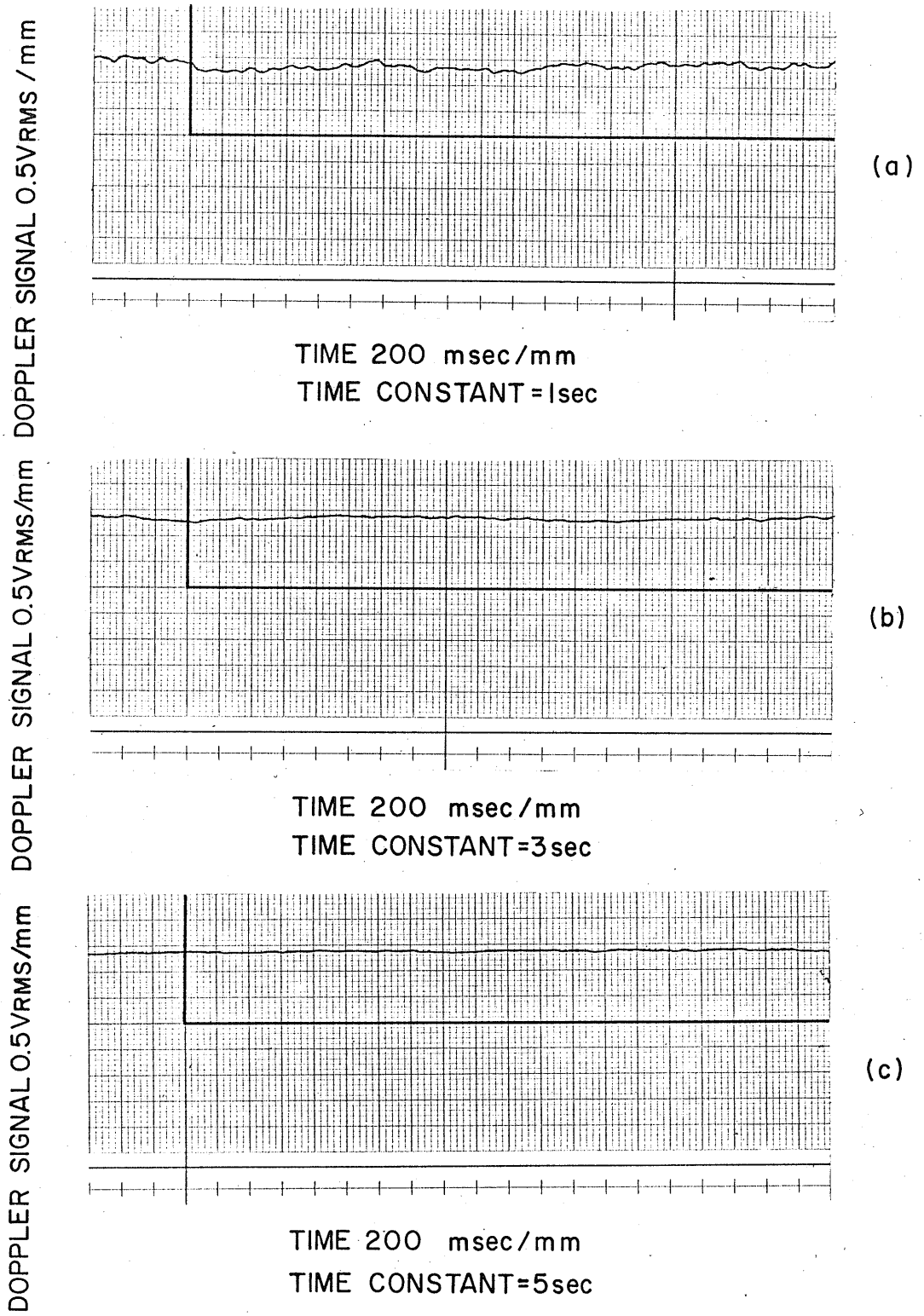

Figure 5.6 (a) Typical Recordings of the RMS Value of the Doppler Signal Averaged for 1 sec
(b) Typical Recordings of the RMS Value of the Doppler Signal Averaged for 3 sec
(c) Typical Recordings of the RMS Value of the Doppler Signal Averaged for 5 sec

[Average bulk density = 113.3 kg/m^3]

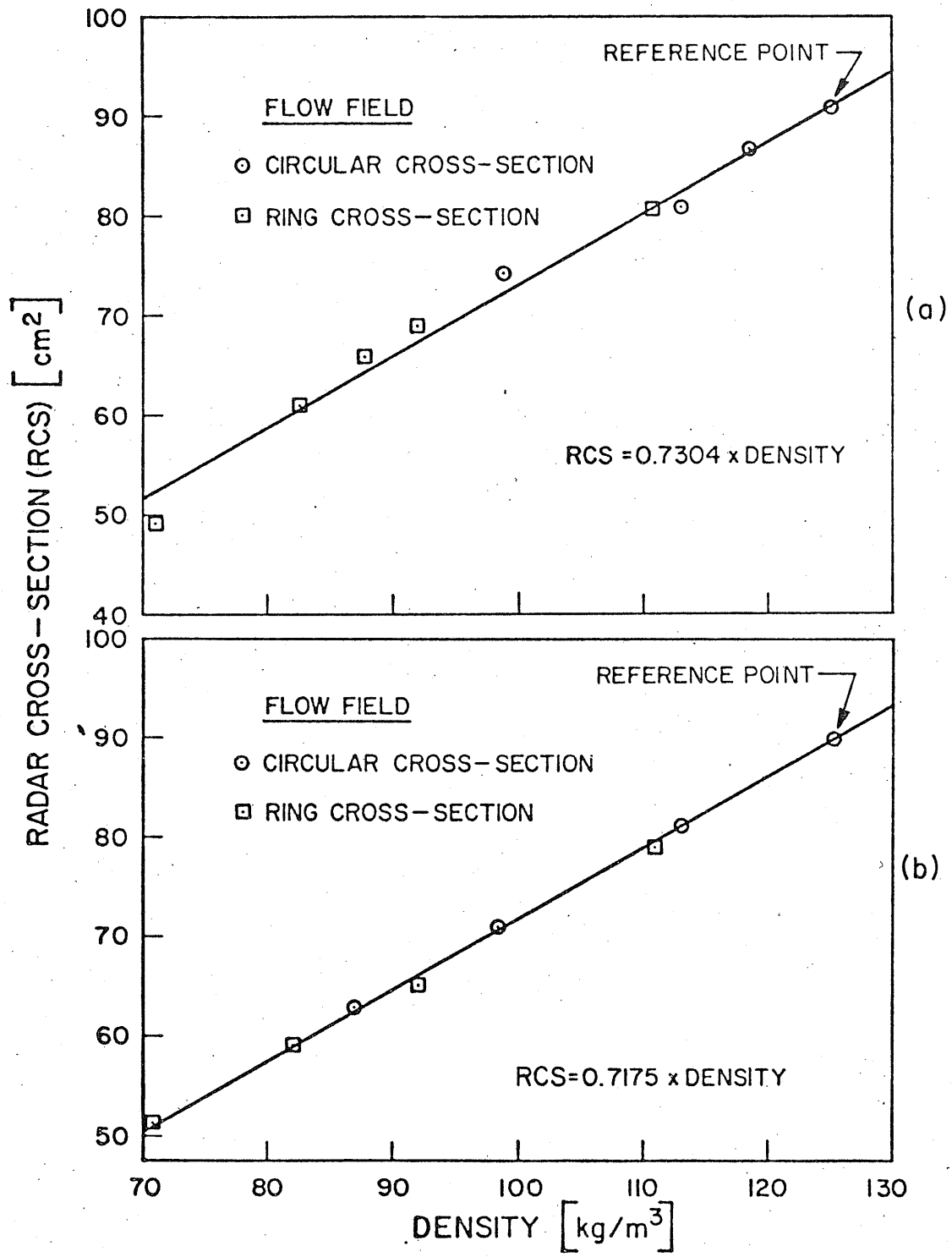

Figure 5.7 (a) RCS as a Function of the Average Bulk Density of Wheat by Analog Signal Processing Technique
(b) RCS as a Function of the Average Bulk Density of Wheat by Digital Signal Processing Technique

investigate the effect of the distribution of particles in the flow field on the RMS value of the Doppler signal. As the Doppler signal voltage depends upon the number of scattering particles moving across the antenna beam, as long as the shape of the flow field is circular, and regardless the air spaces between them, it was found that the RCS of a hollow column of grain also varies linearly with the density. The RMS deviation of the experimental points from the straight line calculated by least squares analysis is equal to 0.23 percent.

The slopes of the characteristic i.e., RCS versus average bulk density of wheat (processed by analog technique) calculated by least squares analysis for different flow field shapes are listed in Table 5.4. As the difference between the slopes for circular and ring cross-section flow fields is very small, therefore, the experimental values for circular and ring cross-section flow fields were combined to calculate the slope of the characteristic shown in Fig. 5.7(a). The experimental points of RCS for circular and ring cross-section flow fields of wheat versus their average bulk densities are plotted in Fig. 5.7(a) for the purpose of comparison. The experimental points fell reasonably well on the straight line calculated for both flow fields. The aforementioned discussion leads to the conclusion that there is no appreciable effect of the distribution of particles on the RMS value of the Doppler signal.

(c) Elliptical Cross-section Flow Field - Experiments were also conducted with the flow field of elliptical cross-section. The major axis of this flow field was 6.2 cm and the minor axis 3.6 cm. The purpose of these experiments was to investigate the effect of change in shape of the flow field. Figs. 5.8(a), (b), and (c) show typical recordings of the RMS value of the Doppler signal for three different relative positions of the flow field in respect to the antenna beam.

TABLE 5.4

Slopes of the Characteristics (RCS Versus Average Bulk Density of Wheat Processed by the Analog Technique) Calculated by Least Squares Analysis For Different Flow Fields.

Shape of the Flow Field	Slope	Difference (%)
Circular Cross-section	0.7317	+0.18
Ring Cross-section	0.7289	-0.20
Circular and Ring Cross-section	0.7304	---

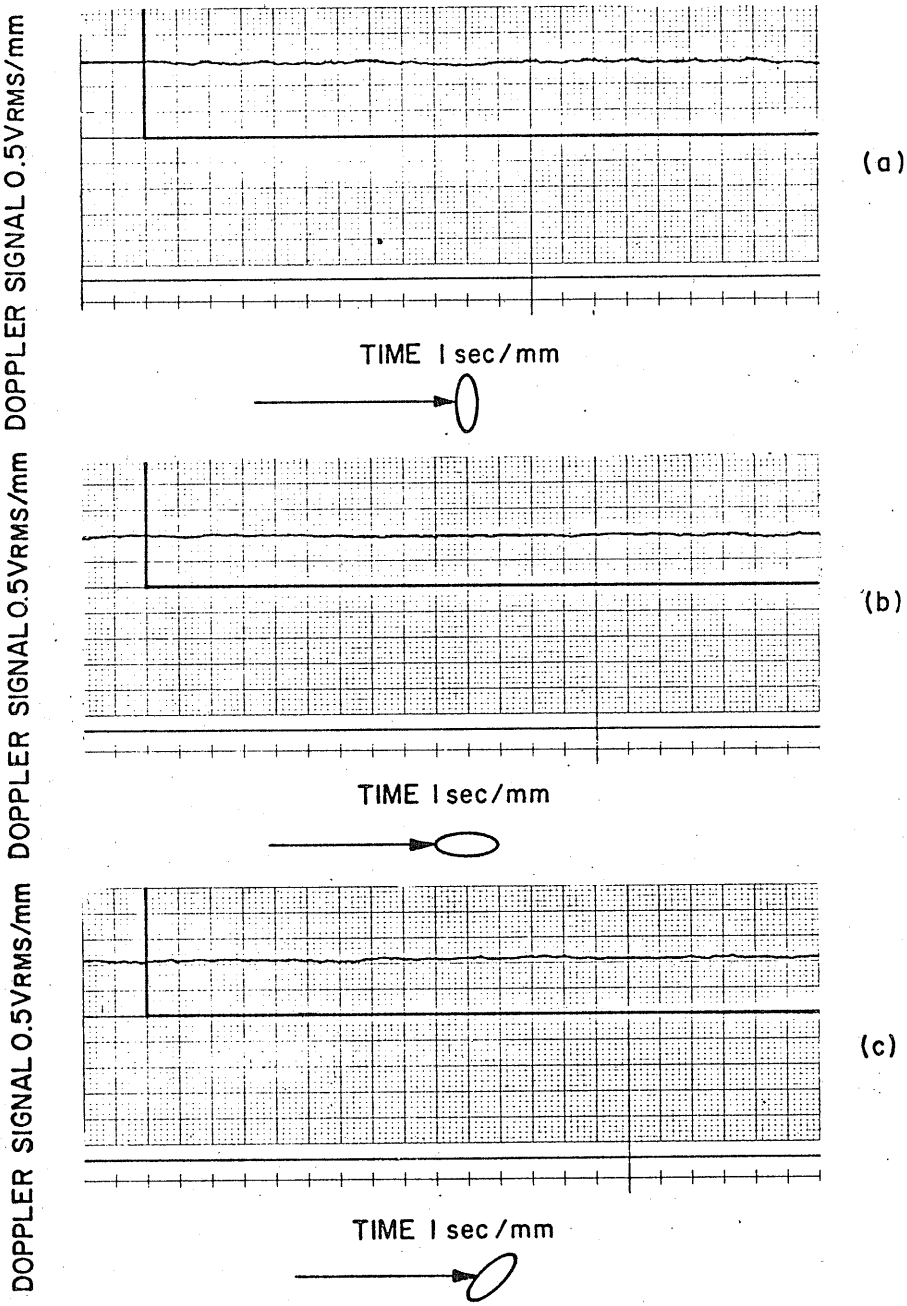

Figure 5.8 (a) Typical Recordings of the RMS Value of the Doppler Signal for the Antenna Beam Parallel to the Minor Axis of the Flow Field

(b) Typical Recordings of the RMS Value of the Doppler Signal for the Antenna Beam Parallel to the Major Axis of the Flow Field

(c) Typical Recordings of the RMS Value of the Doppler Signal for the Antenna Beam at an Angle of 45° to the Major Axis of the Flow Field

[Average bulk density = 110 kg/m^2 Time constant = 3 sec]

Fig. 5.8 indicates that the Doppler signal depends on relative positions of the elliptical flow field in respect to the antenna beam. It is appreciably larger, i.e., 700 mV at the average bulk density of 110 kg/m^3, when the antenna beam is parallel to the minor axis of the flow field, compared with 500 mV and 550 mV when the antenna beam is parallel to the major axis and at an angle of 45° to the major axis of the flow field, respectively. Similar results have been reported (Crispin and Moffett, 1965). It was concluded that the RCS of an elliptical ogive varied with its orientation in the antenna beam.

5.5.4 Digital Signal Processing Technique

(a) Power Spectrum - Doppler signals recorded on the magnetic tape for the continuous flow experiments of wheat, were amplified and fed into a laboratory digital computer (DEC PDP-11) and were digitized at a rate of 2000 points per second. As indicated in 5.5.3(a) 3 sec time averaging gives satisfactory results. Therefore, a group of 6144 samples were analysed by digitizing six adjacent 1024-sample time windows. For illustration Fig. 5.9 shows 1024 points of a digitized Doppler signal fed to the computer.

The fast Fourier transforms were performed on Doppler signals to convert them from the time to the frequency domain. Then the power spectrum was calculated again using the software of the computer (SPARTA). The program designed to perform the FFT and power spectrum using SPARTA LAB Applications-11 is given in the Appendix. The area under the power spectrum which is equal to the square of the RMS value of the Doppler signal was also determined. Table 5.5 shows the average area under the power spectrum curve calculated using the 6144 samples. Inspection of Table 5.5 shows that the differences between the area under the power spectrum for the first group of 6144 samples and the next group taken from the same signal are small. The differences are

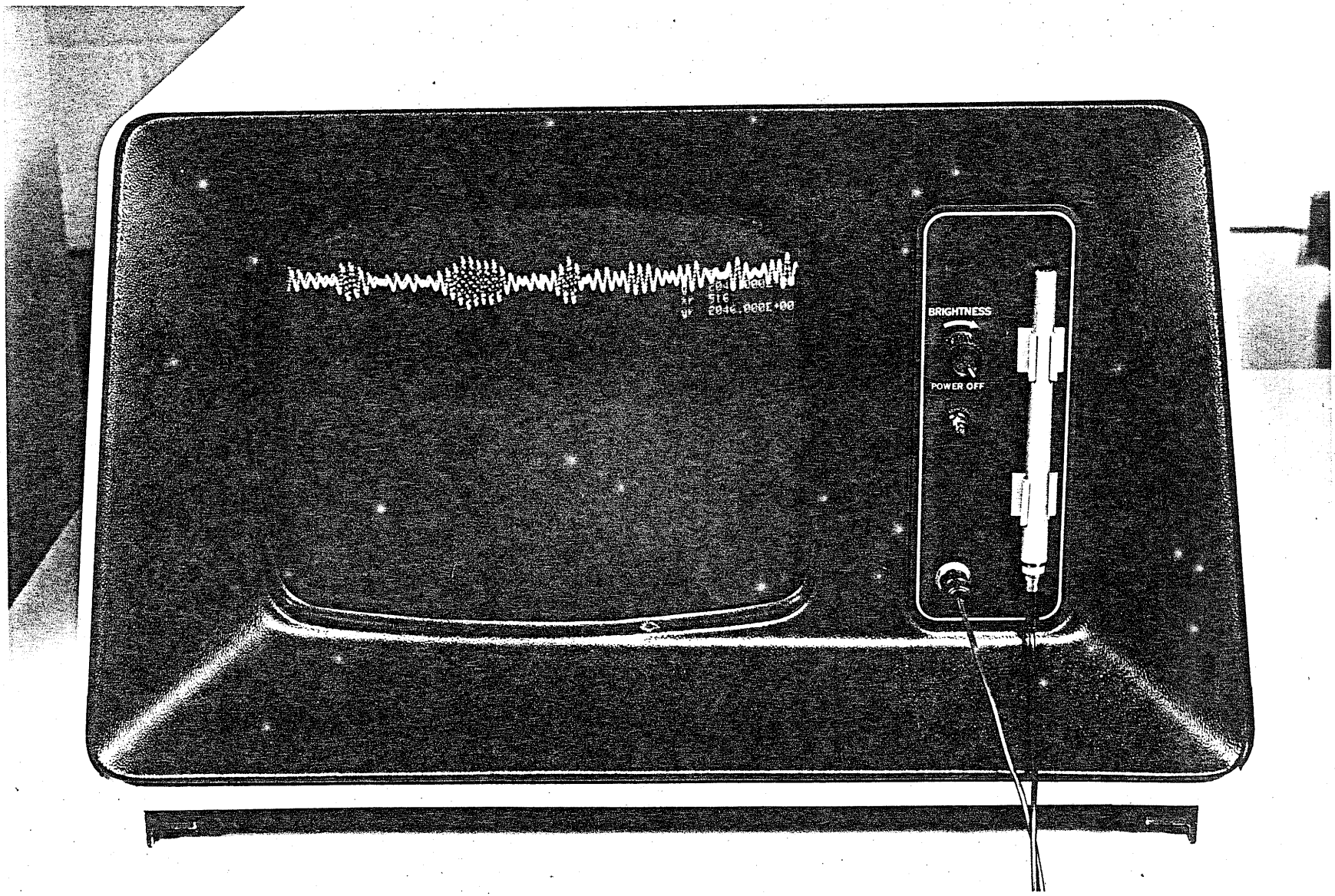

Figure 5.9 Diagram Showing 1024 Points of a Digitized Doppler Signal Fed to the Computer

TABLE 5.5

Area Under the Power Spectrum Curve of the Doppler Signal for Different Bulk Densities

Average Bulk Density (kg/m^3)	Samples of the Digitized Doppler Signal	Average Area (Arbitrary Units)
88.0	1 - 6144	1795573
	6145 - 12288	1742561
98.7	1 - 6144	2014235
	6145 - 12288	2023204
113.3	1 - 6144	2310703
	6145 - 12288	2293652
125.3	1 - 6144	2564762
	6145 - 12288	2495225
71.0*	1 - 6144	1432412
	6145 - 12288	1441040
82.7*	1 - 6144	1690115
	6145 - 12288	1649670
92.0*	1 - 6144	1831226
	6145 - 12288	1844613
110.8*	1 - 6144	2173501
	6145 - 12288	2279443

*Ring cross-section flow field

due to the fact that the Doppler signal varies as a result of variations in the flow field of wheat. Fig. 5.10 depicts a typical power spectrum of the Doppler signal shown in Fig. 5.9.

(b) Determination of the Mean Frequency From the Power Spectrum - The power spectrum depicted in Fig. 5.10 shows clearly that the Doppler signal is not a single discrete frequency, which one would expect for a parallel antenna beam and a single scattering particle, but contains other frequencies spread within a certain band. The spread of the Doppler frequencies is well known for Doppler radar in navigation (Berger, 1957). In the reported experiments the spread of Doppler frequencies results from the divergent antenna beam, the presence of multiple scattering particles with random orientations and from increasing velocity in the free falling flow field.

Various techniques such as short-time autocorrelation (Schulthesis et al., 1954), frequency discriminations or zero crossing counting (Ehrman, 1954), have been employed for the mean frequency measurement of a random signal, and the methods based on these techniques have been studied. The mean frequency of the Doppler signal was determined from the power spectrum. Since the power spectrum is characterized by a regular distribution, a frequency corresponding to the peak value of the curve was taken as a mean frequency. Table 5.6 shows a comparison of average Doppler frequencies as determined from power spectra and measured by the frequency counter method. Table 5.6 shows that the mean Doppler frequencies determined from the power spectrum are always higher than the average Doppler frequencies measured by the frequency counter method. The average shift is equal to 8.8 percent.. This effect is probably due to the fact that the material falls under gravity and the velocity increases as it passes across the antenna beam. In other words, there exists a velocity gradient within

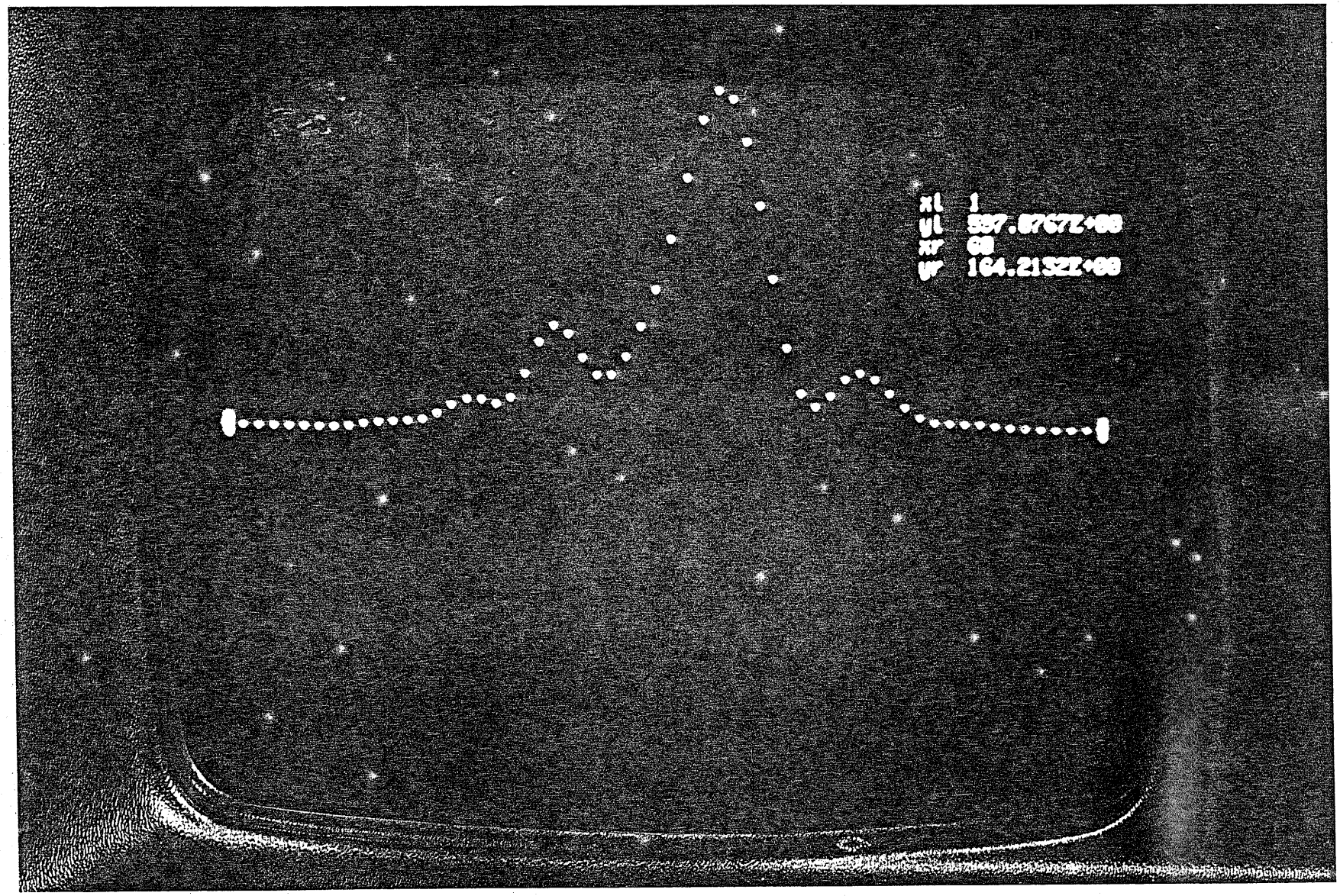

Figure 5.10 Typical Power Spectrum of the Doppler Signal Shown in Fig. 5.9

the antenna beam. This problem of mean frequency shift has also been studied in measurements of gradients of fluid velocities in tubular flow fields by spectral analysis of the signal from a laser Doppler flowmeter (Edwards et al., 1970). Fig. 5.11 shows a typical power spectrum of the Doppler signal, where the cursors indicate the mean frequencies determined by the two methods discussed.

TABLE 5.6

Comparison of Mean Frequencies Measured by the Frequency Counter Method and Calculated From Power Spectra

Average bulk density (kg/m^3)	Mean frequency measured by the frequency counter (Hz)	Mean frequency measured on power spectrum curve (Hz)	Difference from the average shift (%)
125.3	118.7	129.1	1.4
118.4*	117.9	130.8	-0.4
113.3	118.2	129.6	0.7
110.8*	118.8	131.4	-0.3
98.6	118.4	131.6	-0.6
92.0*	118.3	130.7	-0.08
87.8	118.2	132.5	-1.4
71.0*	118.1	129.8	0.4

*Ring Cross-section Flow Field

(c) Width of the Spectrum - The discussion in the previous section leads to the conclusion that Doppler signals are not of a single discrete frequency but contain spectra of frequencies. The width of the Doppler spectrum is given by eq. 3.2

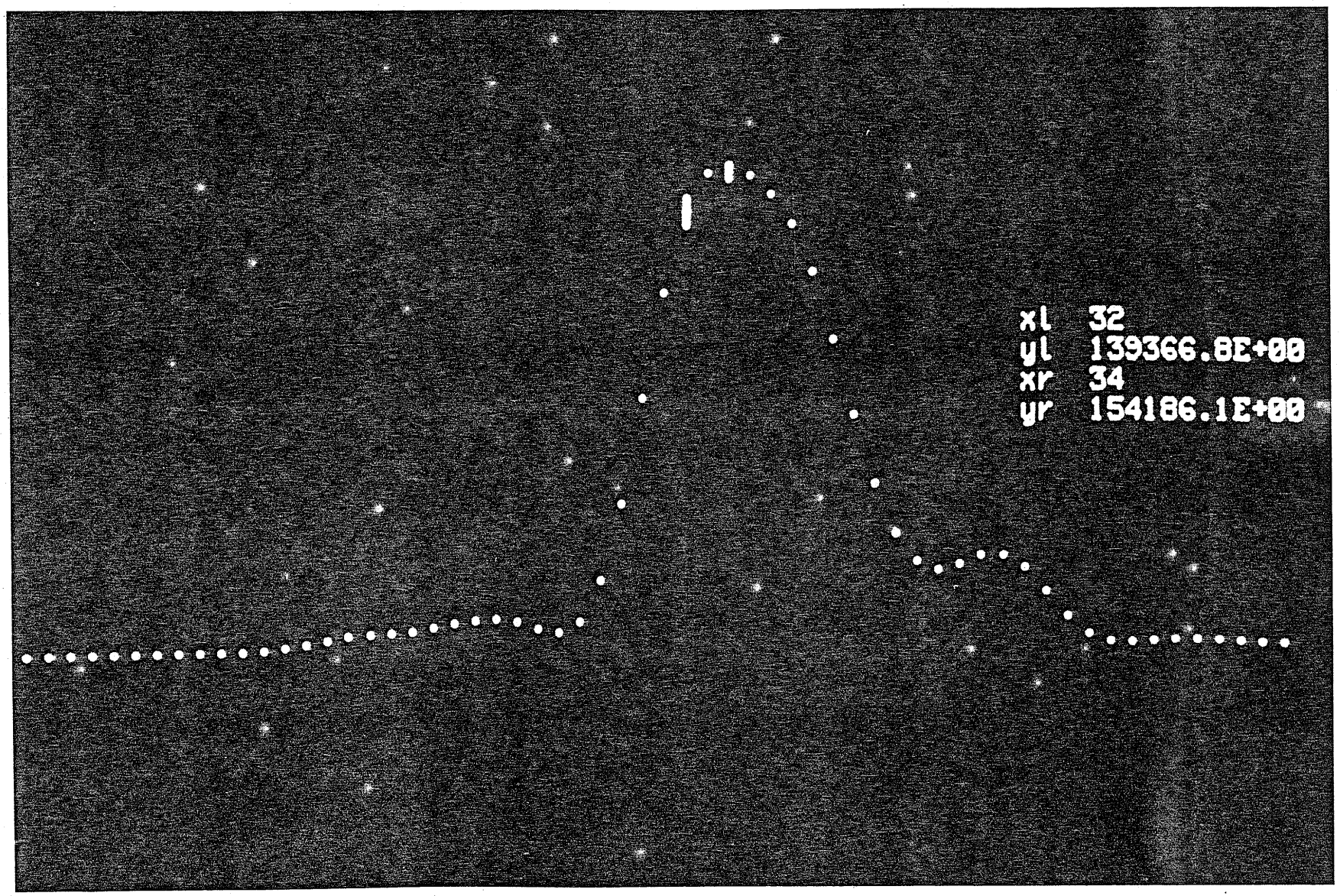

Figure 5.11 Typical Power Spectrum of the Doppler Signal Showing Positions of Cursors for the Mean Frequencies Determination by Two Different Methods

$$\Delta f_d = \frac{2v}{\lambda} \left[\cos\left(\theta - \frac{\Delta\theta_2}{2}\right) - \cos\left(\theta + \frac{\Delta\theta_2}{2}\right)\right] \qquad (5.11)$$

where $\Delta\theta_2$ is the two way, 3dB beamwidth. The other symbols carry the same meaning as in eq. 3.2.

The standard deviation is

$$\delta_{f_d} = \frac{\Delta f_d}{2} \cong \frac{v}{\lambda} \Delta\theta_2 \sin\theta$$

where λ is the free space wavelength in m, v is the velocity vector magnitude in m/sec, θ is the angle between the velocity vector and the centre of the antenna beam in degrees. Table 5.7 gives a comparison of widths of Doppler spectra and standard deviations calculated theoretically and determined from power spectra obtained experimentally.

TABLE 5.7

Comparison of the Theoretical Half Power Spectral Width Δf_d and Standard Deviation δ_{f_d} with Experimental Values Determined from Power Spectra

Theoretical* Δf_d = 21.8 Hz Theoretical* δ_{f_d} = 10.9 Hz

Average Bulk Density (kg/m^3)	Experimental Δf_d (Hz)	Experimental δ_{f_d} (Hz)	Difference Between Experimental and Theoretical δ_{f_d} (%)
125.30	20.3	10.2	- 6.4
98.67	19.8	9.9	- 9.2
87.86	19.5	9.8	-10.0
82.68**	23.8	11.9	+ 9.2

*Calculated assuming 12° as 3 dB points for the antenna utilized in these experiments

**Ring cross-section flow field

(d) Radar Cross-section Versus Area Under Power Spectrum Curve - The area under the power spectrum curve was determined by a digital computer (DEC PDP-11) using software of the computer (SPARTA). As indicated in eq. 3.10 Simpson's formula was used to calculate the area.

As shown in 3.5.2 the RCS of columns of wheat having different bulk densities were calculated using the area under power spectrum curves of the Doppler signal from a metallic calibrating sphere used as a standard cross-section and comparing it with the area under power spectrum curve of Doppler signal from the target of interest.

The slopes of the characteristic i.e., RCS versus average bulk density of wheat (processed by the digital technique) calculated by least square analysis for different flow field shapes are listed in Table 5.8. It is evident from Table 5.8 that the difference between the slopes for circular and ring cross-section flow fields is very small. Therefore, the experimental points for both flow fields were combined to calculate the slope of the final characteristic. The values of the RCS as a function of average bulk densities of wheat calculated from the spectra are plotted in Fig. 5.7(b). Fig. 5.7(b) shows clearly that experimental points for both flow fields fell reasonably well on the straight line calculated by the least squares technique. This verifies the thesis that the RCS of a column of grain depends linearly on the average bulk density of the particulate solids.

TABLE 5.8

Slopes of Characteristics (RCS Versus Average Bulk Density of of Wheat Processed by the Digital Technique) Calculated by Least Square Analysis for Different Flow Fields

Shape of the Flow Field	Slope	Difference (%)
Circular Cross-section	0.7201	+0.36
Ring Cross-section	0.7139	-0.50
Circular and Ring cross-section	0.7175	---

CHAPTER VI

CONCLUSIONS

A need for accurate measurements of mass flow rates of particulate solids in agriculture as well as in other industries was pointed out and the potential for a flowmeter working on the principle of the Doppler effect was considered in some greater detail. It is evident from this research that a Doppler radar flowmeter can measure continuously the mass flow rate of particulate solids in hostile environments and difficult situations with good accuracy. The main advantages of the meter are that it does not require any mechanical probe to be introduced into the flow field, contains no moving parts and hence is obstructionless. If the cross-sectional area of the flow field, which depends upon the calibration of the flowmeter, is known, the mass flow rate can be computed by multiplying the average bulk density, by the average bulk velocity and by the cross-sectional area of the flow field.

The bulk density of the wheat used in the experiments was determined by a direct weighing technique. The uncertainty found in the measurement of the bulk density by this method was not more than 6 percent in any case.

A monostatic configuration was employed throughout the experiments using a viewing angle of 42.5°. An advantage of the monostatic configuration is that only one site is required as compared with the two sites of the bistatic configuration, which makes the flowmeter more economical and suitable for industrial applications.

Doppler signals from the flowmeter were analysed by two independent processing systems: an analog system (on line) and a digital system (off line). It was found that due to semi-random movements of particles in the flow field,

the Doppler signals were of a very complex waveform and instantaneous signals did not accord any useful indication about the density of particulate solids. However, an integration time of 3 seconds was found appropriate to extract informations about the average bulk density of granular material from the Doppler signal. The power spectrum of the Doppler signals provided important information about the parameters of the flow field. The average area under the power spectrum curve which is equal to the square of the RMS value of the digitized Doppler signal was found proportional to the average bulk density of particulate solids. The mean Doppler frequency which is proportional to the average bulk velocity of the flowing material was found shifted, for all investigated flow rates, by about 9 percent in respect to the frequency of the peak of the power spectrum.

High accuracy, fast response, no obstructions in the flow field, linearity over wide ranges of velocities and bulk densities, suitability for different granulations of particulate solids, absence of moving parts, simplicity and low cost make this flowmeter a versatile instrument for a variety of industrial applications.

REFERENCES

(1) Albright, R.J. and J.H. Harris. 1975. Diagnosis of urethral flow parameters by ultrasonic backscatter. IEEE Trans. on Biom. Engineering. 22:1-11.

(2) Andrian, R.J. and R.J. Goldstein. 1971. Analysis of a laser Doppler anemometer. J. of Physics E. Scientific Instruments. 4:505-511.

(3) Arts, M.G.J. and J.M.J.G. Roevros. 1972. On the instantaneous measurement of blood flow by ultrasonic means. Med. and Biological Engineering. 10:23-24.

(4) Beck, M.S., J. Drane, A. Plaskowski and N. Wainwright. 1968. A new method of measuring the mass flow of powder in a pneumatic conveyor using an on-line computer. Instr. Elec. Engrg., London, England, Conference Publ. n43:133-147.

(5) Beck, M.S. and N. Wainwright. 1969. Current industrial methods for solid flow detection and measurement. Powder Technol. 24:189-197.

(6) Berger, F.B. 1957. The nature of Doppler velocity measurement. IRE Trans. ANE. 4:103-112.

(7) Bragg, G.M. 1974. Treatment of results. p. 76-85 in Principles of Experimentation and Measurement. Prentice-Hall, Inc. Englewood Cliffs, New Jersey.

(8) Brody, W.R. and J.D. Meindi. 1974. Theoretical analysis of the CW Doppler ultrasonic flowmeter. IEEE Trans. on Biom. Engineering. 21:183-192.

(9) Brown, S.G., T.M. Bates and J.E. Wilhelm. 1962. Flame monitoring and combustion stability. ASME Paper 62-WA-186.

(10) Chugh, R.K., S.S. Stuchly and M.A. Rzepecka. 1972. Dielectric properties of wheat at microwave frequencies. Trans. of ASAE, 16(5):906-909, 913.

(11) Cooley, J.W. and J.W. Tuckey. 1965. An algorithm for the machine calculation of complex Fourier series. Math. of Comput. 19:297-301.

(12) Crispin, J.W. and A.L. Maffett. 1965. Radar cross section estimating for simple shapes. IEEE Proc. 53(8):833-848.

(13) Craven, G.F. 1964. Automatic weighing and batching of bulk solids. Chem. and Process Eng. 45:125-128.

(14) Dean, S.K. 1955. Flowmeter for granular materials. Engineering 179(4654):430-431.

(15) DISA 1973. Bibliography of laser Doppler anemometry literature. DISA Electronics A/S, DK-2730, Herlev, Denmark.

(16) Edwards, R.V., M.J. French and J.W. Dunning. 1971. Spectral analysis of the signal from laser Doppler flowmeter. J. of Applied Phys. 42:837-850.

(17) Ehrman, L. 1964. Analysis of a zero-crossing frequency discriminator with random inputs. IEEE Trans. ANE 12:113-119.

(18) Ellerbruch, D.A. 1970. Microwave methods for cryogenic liquid and slush instrumentation. IEEE Trans. IM 19(4):412-416.

(19) Goldstein, R.J. and D.K. Kried. 1967. Measurement of laminar flow development in a square duct using a laser-Doppler flowmeter. J. Appl. Mech. 34:813-818.

(20) Hamid, A. 1975. Microwave Doppler-effect flow monitor. M.Sc. Thesis, Univ. of Manitoba, Winnipeg, Canada.

(21) Hannir, J. 1970. Radascan flow/no flow detector. Measurement and Control 3(12):356.

(22) Harris, J. 1970. Integrating flow fields with radar and laser sources. Measurement and Control 3(11):188-192.

(23) Henderson, J.M. 1966. A mass flowmeter for granular material. ISA Trans. 5:78-83.

(24) Holman, J.P. 1971. Analysis of experimental data. p. 37-39 in Experimental Methods for Engineers. McGraw-Hill Book Company, New York.

(25) Hooper, A.W., B. Ambler and M.T. Hughes. 1974. Design and development of a combine harvester discharge meter. Unpublished Research Work in National Institute of Agric. Engineering, Silsoe, Bedford.

(26) Hyltin, T.M., T.D. Fuchser, H.B. Tyson and W.R. Regueiro. 1973. Vehicular radar speedometer. SAE Publ. No. 730125 Cobo. Hall-Detroit, MI.

(27) Kirwan, J.O. and L.E. Demler. 1955. Continuous weighing and feeding. Instr. and Automation 28:98-101.

(28) Kobayashi, M., H. Osawa, N. Morinaga and T. Namekawa. 1974. On the mean frequency measurement system using correlation detection. IEEE Trans. AES 10:364-371.

(29) Lab applications-11, system reference manual. 1974. Digital Equipment Corporation, Maynard, Massachusetts.

(30) Marshal, J.S. and W. Hitschfeld. 1953. The interpretation of fluctuating echo from randomly disturbuted scatterers. Canadian Journal of Physics. 31:962.

(31) Nelson, S.O. 1972. Frequency dependence on the dielectric properties of wheat and the rice weevil. Ph.D. Dissertation, Iowa State University, Ames, Iowa.

(32) Pawula, R.F. 1968. Analysis of an estimator of the centre frequency of a power spectrum. IEEE Trans. IT 14:669-676.

(33) Parker, R.R. 1970. A microwave Doppler flowmeter. MIT Report 2-8-141.

(34) Peripherals handbook, program interfacing, PDP-11. 1973. Digital Equipment Corporation, Maynard, Massachusetts.

(35) Schultheiss, P.M., C.A. Wogrin and F. Zweig. 1954. Short time frequency measurement of narrow-band random signals in the presence of wide-band noise. J. Appl. Phys. 25:1025-1036.

(36) Skolnik, M.I. 1962. Introduction to radar systems. McGraw-Hill Book Company, New York.

(37) Stuchly, S.S., M.S. Sabir and A. Hamid. 1975. A system for monitoring mass flow of grain. ASAE Paper No. 75-303. Fargo, North Dakota.

(38) Stuchly, S.S., A. Hamid and M.S. Sabir. 1975. A continuous and contactless system for monitoring velocity of grain flow. CSAE Paper No. 75-104, Brandon University, Brandon, Manitoba.

(39) Valenti, F. 1961. The automation of free flowing solids. Can. Mining Met. Bull. 45:833.

(40) Webb, A.S., Stone, Webster Eng. Corp. 1974. Electromagnetic Flowmetering Instrumentation Technology. (March 1974): 29-36.

(41) Yeh, H. and H.Z. Cummins. 1964. Localized fluid flow measurements with an He-Ne laser spectrometer. Appl. Phys. Lett. 4:176-178.

APPENDIX

A computer program was developed for calculating the power spectrum of Doppler signals using software package (SPARTA) of the digital computer PDP-11. The program is given as follows:

```
R  ADRK05
* MSDAT1/R!5/S! 13304=
R  GSPART
BBU S2 F1 1024
MOP
MSDAT1
MIN S1 1024 1 I1
DDI S1
DLO
BSU S2 S2
FFT S1
FPO S1 S 2 F1
MCL
MOP
 T1=
MOU F1 01
MCL
BSU F1 F1
MOP
=T1
SAD F1 1000000
MIN F1 60 30 I1
DDI F1 60
DCU
DCV
BSM NP
BIN F1 A
```